2017-01-01

Behavior of Sandwich Composite Cores under Extreme Conditions

Carlos Daniel Garcia Perez
University of Texas at El Paso, carlosdanielgarcia5@hotmail.com

BEHAVIOR OF SANDWICH COMPOSITE CORES UNDER EXTREME CONDITIONS

CARLOS DANIEL GARCIA PEREZ

Master′s Program in Mechanical Engineering

APPROVED:

Pavana Prabhakar, Ph.D., Chair

Yirong Lin, Ph.D.

David Roberson, Ph.D.

Charles H. Ambler, Ph.D.
Dean of the Graduate School

to my

Family and Friends

BEHAVIOR OF SANDWICH COMPOSITE CORES UNDER EXTREME CONDITIONS

by

CARLOS DANIEL GARCIA PEREZ

THESIS

Presented to the Faculty of the Graduate School of

The University of Texas at El Paso

in Partial Fulfillment

of the Requirements

for the Degree of

MASTER OF SCIENCE

Master′s Program in Mechanical Engineering

THE UNIVERSITY OF TEXAS AT EL PASO

August 2017

Acknowledgements

I would like to give thanks to my advisor, Dr. Pavana Prabhakar from the Mechanical Engineering Department at The University of Texas at El Paso, for her advice, patience and constant support through my master. It has been a pleasure and a priviledge to work under her expert technical guidance and support.

Additionally, I want to thank all my friends for their support during this process and have been in every step of my educational process: Raudel Avila, Alejandra Castellanos, Alan Esparza, Jesus Gerardo Reyes, Ricardo Garcia, Tania Ventura and all the Manufacturing and Mechanics Lab (MaMel). Thank you guys for all your support. Finally, I wish to express my deepest gratitude to my parents and brother for their support through out all these years.

Abstract

The use of composite structures for diverse applications have become of great interest for scientists and engineers thanks to the advantages that they may offer in comparison to conventional materials. In the case of sandwich composite structures, its mechanical properties can be tailored according to the necessities through the correct selection of a core and facesheets. In combination, this "new" material will have superior properties compared to traditional materials such as steel and aluminum. For arctic exploration, a core with low moisture absorption, low density, and resistance to extreme, low temperatures is desirable for this type of application. This thesis describes the process of exposing two distinct types of foam cores under arctic conditioning (-60^{o}C) and sea water exposure in order to analyze the impact that this type of environment may have in the mechanical response of the foam cores. Polyvinyl Chloride foams cores were condition under sea water, arctic temperatures, and in combination in order to analyze its compressive response. Epoxy/Cenosphere syntactic foams were subjected to arctic temperatures followed by compression and flexural tests. It was observed that long term sea water conditioning along with arctic exposure can be detrimental to the mechanical properties of PVC foams as well as of syntactic foams.

Table of Contents

List of Tables

List of Figures

Chapter 1

Introduction

Advances in technology had driven the evolution of humanity through centuries. In recent years, the demand for new and better technology has increased. Society always want to have the latest and best innovations. They want a more resistant cellphone while it remains lightweight, to drive a fuel efficient vehicle, or to be able to explore places under extreme conditions.

This constant evolution of technology has led to the necessity to explore new materials. It is difficult to be able to obtain better performance using the same traditional materials that has been employed for many years. Therefore, materials such as polymers, ceramics, and composites have become attractive replacements for conventional materials such as aluminum and steel. Composite materials, for example, have existed in nature for many years but they started to gain popularity during 1980 [1] due to its mechanical properties and its ability to tailor them for specific applications. Composites materials come from the combination of two or more materials with different properties. Through the combination of these material, improvements in the mechanical response of the newly formed material can be obtained such as higher strength, modulus, bending stiffness, and chemical resistance [2].

Every year, more and more composite materials replace conventional materials thanks to its improved mechanical properties. Sectors such as aeronautics, transportation, and marine exploration understand the advantages of utilizing composite materials over conventional materials leading to the implementation these materials in many of its applications/structures.

1.1 Sandwich Structured Composites

Sandwich composites have become of great importance to applications such the marine due to its favorable characteristics such as lightweight and ability to tailor its mechanical

properties depending of the requirements of the application. Sandwich composites are primarily composed off three components, facesheets or skins, a core, and an adhesive as it can be seen in Figure 1.1. Typically, facesheets are characterized by being very stiff and thin, while the core is usually thick but lightweight. This two components bonded together by the adhesive provide the basis for a strong and stiff structure.

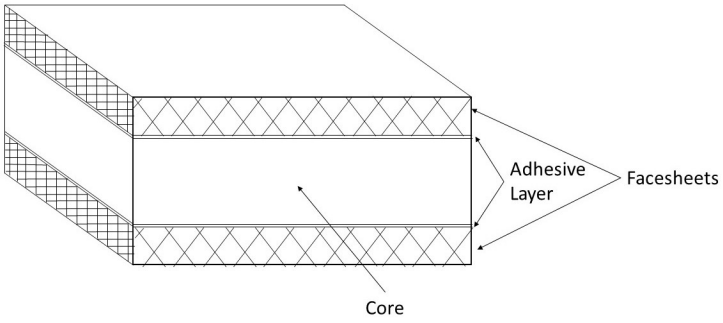

Figure 1.1: Structure of a Sandwich Composite

The properties of the sandwich composites depend mainly in the properties of its two main constituents (facesheets and core), the bonding between both,and the thickness of the structure. Adequate selection of core and skins to conform the sandwich composites may provide an advantage over traditional materials making them suitable for a large number of applications regardless of the environmental conditions. Some of the advantages of implementing sandwich composites may include: low density meaning lightweight, high stiffness, damage tolerance, and and a wide range of choices for the facesheets and cores.

1.2 Cores

Depending of the requirements of the application, distinct core materials can be selected. Some type of cores are wood, foams, honeycomb structure, and non-woven core fabric. They are characterized by being lightweight, having low density, and relatively inexpensive. One of the most common type of cores employed are foam cores. They may be used for high

performance applications where weight is important. In this thesis, two types of foam cores, Polyvinyl Chloride (PVC) Foams and Cenosphere/Epoxy syntactic foams, are proposed for the study as core materials for sandwich structures for marine explorations under extreme, low temperatures due to its ability to withstand low temperatures and its low moisture absorption.

1.3 Scope and Outline of the Thesis

The ability to tailor the properties of a sandwich composites and its strength-to-weight ratio has lead to the implementation of these materials in areas such as aerospace, naval and automobiles applications. The selection of the sandwich composite constituents depends greatly on its application. Resistance to harsh environments without compromising performance is of utmost importance for arctic exploration. Damage resistance to corrosive environments such as sea water and extreme low temperatures are requirements for any material employed for marine, arctic exploration. The performance of Polyvinyl Chloride (PVC) Foams and Cenosphere/Epoxy syntactic foams under the conditions previously mentioned is investigated. First, the influence of arctic exposure has in the response of PVC foams under compressive loading is described in Chapter 2. Afterwards, the compressive and flexural behavior of cenosphere/epoxy syntactic foam under arctic conditions is discussed in Chapter 3 and 4, respectively. Next, a computational model for syntactic foams during compression is presented in Chapter 5. Finally, the thesis concludes with Chapter 6 by summarizing the results of this study with a discussion on future work.

Chapter 2

Influence of Arctic Sea Water on the Compressive Response of Polyvinyl Chloride Foams

2.1 Introduction

Sandwich composites have been replacing traditional materials used in the construction of naval crafts, predominantly due to their lightweight, enhanced performance and affordability. They are typically composed of two thin laminates that are bonded to a lightweight core to provide the basis for a strong and stiff structure. A major concern is the response of these composites when exposed to corrosive sea water environment for extended periods of time. Hence, it is important to determine the extent of degradation experienced by naval materials exposed to harsh environments to assist in improving their damage resistance, tolerance, and life cycles. Further, with an increased interest in arctic explorations, it has become critical to understand the effects of extreme low temperatures on naval structural materials. In the current paper, the focus is on investigating the influence of arctic sea water conditions on the compressive behavior of polymeric foam core material.

Several researchers have characterized the behavior of different polymeric foams under static or dynamic loading without any type of exposure to external environments [3, 4, 5, 6, 7]. Aviles and Aguilar-Montero [8], Shen and Springer [9], and Tagliavia *et al.*[10], among others have investigated the influence of moisture absorption on sandwich foam core materials. Further, experimental investigations have addressed the degradation of mechanical properties of foam core materials due to the exposure to sea water conditions [11, 10, 12, 13, 14]. The work by Nordin *et al.* [12] discusses the effect of exposure to low temperatures over a long period of time on the stiffness of glass fiber composites.

Other studies have shown that exposure to low temperature may increase the strength and stiffness of the foam material, but the exposure to sea water caused a degradation in

the shear properties [11, 15]. In the study performed by Siriruk *et al.* [11], a reduction of about 3% was observed in tensile modulus due to sea water conditioning, while samples exposed to low temperatures did not show any effect. Also, in the same study, a reduction between 5% and 8% was observed in the shear modulus due to sea water conditioning and a combined conditioning of sea water and low temperature. In a study conducted by Singh and Davidson [15], it was shown that an increase of 24% in the static strength of sandwich composites was observed with reduction in temperature, as well as an increase in fatigue life.

Nevertheless, seldom work has been reported that discusses the effects of arctic temperatures, sea water, and combined conditions on foams. With the overarching goal of improving the performance of sandwich composites in arctic sea water conditions, the focus of the work presented here is on polyvinyl chloride (PVC) foams that are used as core materials in sandwich composites for marine construction. The objective of this paper is to investigate the effects of sea water absorption and arctic environment on the in-situ arctic compressive properties of PVC foams.

This paper is organized in the following sections: A brief description of the material investigated and specimen dimensions is provided, followed by a description of the types of conditions that the test samples were subjected to. The methods used to determine the water absorption content in the samples are explained next along with a discussion on the coefficient of diffusion. Then, a description of the process to expose the samples to sea water and condition them in arctic environment is given. Further, testing methodology and analysis to determine the compressive modulus and strength are described. Finally, a comparison between the serval combinations of environmental conditions on the compressive properties of PVC foams is discussed, followed by conclusions.

2.2 Experimental Approach

2.2.1 Materials and Specimens

Divinycell H45 (supplied by fibreglast.com), is a closed-cell PVC foam with nominal density of 45 kg/m^3, which corresponds to its nomenclature H45. Mechanical properties of this PVC foam provided by the manufacturer are listed in Table 2.1[16]. Divnycell H45 is a rigid PVC foam with a closed, inert gas filled cellular structure, was considered in this study due to its potential naval application for sandwich composites accounting for low water absorption. Specimens were cut from panels using a feather cut machine powered by a thermal generator. First, the foam panel was measured and marked to desired specimen dimensions. Then, the feather cut bow was held vertically and the foam sheet was cut along the marked lines using gravity. Finally, the edges of the specimens were sanded to eliminate any possible burnt material surfaces caused during the cutting process. The dimensions of flatwise compression test specimens were set to be 75 mm long x 75 mm wide x 12.7 mm thick in accordance with the ASTM standard C365 [17]. Specimens were divided into sets of 5 and labeled based on the type of conditioning to which they were going to be exposed and in-situ testing conditions. ASTM standards C272 [18] and D5229 [19] were used as guidelines for water absorption study in addition to the ASTM C365 [17] to determine the dimensions of the specimens.

Table 2.1: Properties of Divinycell H45 Foam

Property	Unit	H45
Density	kg/m^3	48
Tensile Strength (ASTM D 1623)	MPa	1.4
Tensile Modulus (ASTM D 1623)	MPa	55
Compressive Strength (ASTM D 1621)	MPa	60
Compressive Modulus (ASTM D1621-B-73)	MPa	50
Shear Strength (ASTM C 273)	MPa	0.56
Shear Modulus (ASTM C 273)	MPa	15

2.2.2 Environmental Conditioning and In-situ Testing Conditions

Specimens were subjected to five different types of environmental conditioning as follows: (i) dry room temperature condition, (ii) dry arctic temperature, (iii) synthetic sea water submersion until saturation, (iv) semi-saturation of sea water followed by arctic condition, and (v) synthetic sea water submersion until saturation followed by arctic condition. Details of each of these environmental exposures are discussed in detail in the following sections. Further, compression tests were performed on the exposed samples at room temperature (23^{o}C) and in-situ arctic temperature (-60^{o}C).

In order to follow the type of environmental conditioning and in-situ testing environment for the samples, a naming convention was used as described in Table 2.2. Samples were named according to the naming convention: XYZ. X and Y placeholders represent the combined environmental conditioning of the specimens, where D denotes dry, A demotes arctic temperature, sS denotes semi-saturated and S denotes saturated conditions. Z represents the in-situ testing environment, where A denotes arctic (-60^{o}C) and R denotes room (23^{o}C) temperature. N denotes no environmental conditioning or in-situ testing environment. Overall, there were 8 different cases based on combined environmental conditioning and in-situ testing environment as shown in Table 2.2.

Table 2.2: Overview of test matrix based on combined environmental conditioning and in-situ testing environment

Initial Conditioning	Secondary Conditioning	Test Environment	No. of Specimens	Name Code
Dry	None	RT	5	DNR
	Arctic	RT	5	DAR
	Arctic	Arctic	5	DAA
Semi-Sat	Arctic	RT	5	sSAR
	Arctic	Arctic	5	sSAA
Saturated	None	RT	5	SNR
	Arctic	RT	5	SAR
	Arctic	Arctic	5	SAA

2.2.3 Sea Water Conditioning

Prior to exposing the samples to any type of conditioning mentioned above, they were oven dried at 50^{o}C for 24 hours to eliminate any pre-existing moisture content in the material. The weight and dimensions of the dried specimens were recorded, which were used as baseline measurements. Five specimens were fully submerged and spaced inside a glass tank filled with synthetic sea water for the sea water absorption study. Syntactic sea water used during conditioning was a substitute ocean water without heavy metals, which was purchased from Ricca Chemical Company. According to the manufacturers, the synthetic sea water was prepared in accordance with ASTM D1141[20], which is a standard practice for the preparation of substitute ocean water. Due to the low density of these foams, specimens have the tendency to float when submerged in water. Sealed aquarium gravel bags were used as weights to hold specimens submerged through nylon threads in order to fully submerge them in the synthetic sea water bath. Specimens were immerse horizontally in the container and had a minimum of 25 mm head of water above. ASTM standards C272 [18] and D5229 [19] were used for the conditioning of the foams in synthetic sea water.

Weight gained by each specimen was recorded periodically to determine the extent of water absorption as time progressed. Samples were removed from the water bath individually, excess liquid was wiped off with an absorbent cloth and their weight was recorded immediately. The samples were weighed every 24 hours initially and twice per week later, as the weight gained by the material decreased significantly with time as compared to the initial days. Specimens were weighed until the weight gained was less than 2% of the entire weight gained in the previous intervals, which was an indication of approaching saturation. To determine the water uptake percentage, $M(t)$, by the material at any given time t, the following expression was used:

$$M(t) = (\frac{w(t) - w_0}{w_0}) * 100 \tag{2.1}$$

where, $w(t)$ is the weight at the given time t and w_o is the initial baseline weight.

2.2.4 Arctic Conditioning

To the best of the authors' knowledge, there is no standard to follow for arctic exposure study of foam cores. Due to the lack of a standard to follow, the same initial procedure was followed as in the case of sea water conditioning step. First specimens were oven dried at 50^{o}C for 24 hours. Next, their weight and dimensions were recorded before subjecting them to arctic condition (-60^{o}C). Ten specimens were placed in a Thermo Scientific TSU Series -86^{o}C Upright Ultra-Low Temperature Freezer at -60^{o}C for a period of 48 hours, after which five specimens were tested under room temperature condition (23^{o}C) and five under in-situ arctic condition (-60^{o}C). The procedure followed to obtain the compressive properties for all specimens in this study is discussed in a later section.

2.2.5 Combined Sea Water and Arctic Conditioning

Within the combined sea water and arctic conditioning cases, the samples were first conditioned under synthetic sea water at room temperature followed by arctic exposure. For the water conditioning stage, the same procedure was followed as described in the previous

section on "Sea Water Conditioning". Two sets of samples were prepared, where one set was submerged in synthetic sea water for a specified amount that corresponds to semi-saturation state in the samples, while the second set was submerged until saturation was reached. The number of days required for water saturation and semi-saturation in these samples was determined in the earlier study of "Sea Water Conditioning". The samples were removed from the water tank at saturation and semi-saturation each, weighed and dimensions recorded, followed by placing them in a freezer to simulate arctic conditions at -60^{o}C. Specimens were exposed to -60^{o}C for 48 hours after which they were tested either at room temperature or in-situ arctic temperature.

2.2.6 Compression Tests

Flatwise compression tests for all samples were conducted using Instron 5969 Tabletop Universal Testing System. ASTM standard C365[17] was followed as a guideline to determine the compressive properties. Cross head displacement rate of 0.5 mm/min was used for the tests. For in-situ arctic tests, an Instron environmental chamber was used along with the Universal Testing System. Liquid nitrogen was employed to achieve and maintain the desire temperature in the chamber during testing. The chamber was set to a temperature of -60^{o}C prior to conducting the tests, and the samples were then placed in the environmental chamber for testing. The same ASTM standard was followed for all compression tests under varying environmental conditioning and in-situ testing conditions.

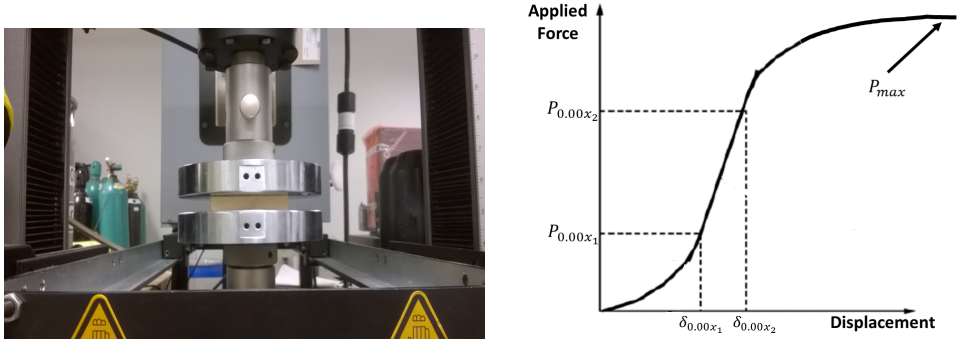

(a) (b)

Figure 2.1: (a)Compression test in progress for a Divinycell H45 Foam sample; (b)Representative load-deflection curve

Flatwise compressive modulus and ultimate strength were calculated using the following equations:

$$E_z^{fc} = \frac{(P_{0.00x2} - P_{0.00x1})t}{(\delta_{0.00x2} - \delta_{0.00x1})A}; \qquad F_z^{fc} = \frac{P_{max}}{A} \tag{2.2}$$

where, E_z^{fc} is the flatwise compressive chord modulus, $P_{0.00x}$ is the applied force at a given deflection, t is the specimen mean thickness, $\delta_{0.00x}$ is the recorded deflection value, A is the cross-sectional area, F_z^{fc} is the ultimate compressive strength, and P_{max} is the ultimate force prior to failure. Figure 2.1(a) shows the experimental setup of a flatwise compression test and Figure 2.1(b) depicts a representative load-displacement response for the test. The linear region chosen for calculating the compressive chord modulus is shown in the the figure. In the following section, results from the exposure studies and flatwise compression tests conducted are discussed in detail.

2.3 Results

2.3.1 Sea Water Uptake and Diffusion

For the saturated and semi-saturated sea water conditioning cases, water uptake was monitored regularly. The moisture content with respect to time was calculated using Equa-

tion 2.1. Representative graph of the water uptake percentage from one of the specimens is shown in Figure 2.2. It was observed that the specimens reached a weight gained equilibrium (average 160.22±8%) after approximately 100 days of sea water exposure. Also, the sea water uptake demonstrated Fickean behavior, which consists of an early stage linear increase in slope followed by a gradual decrease over time until it reaches a plateau region indicating the first signs of saturation.

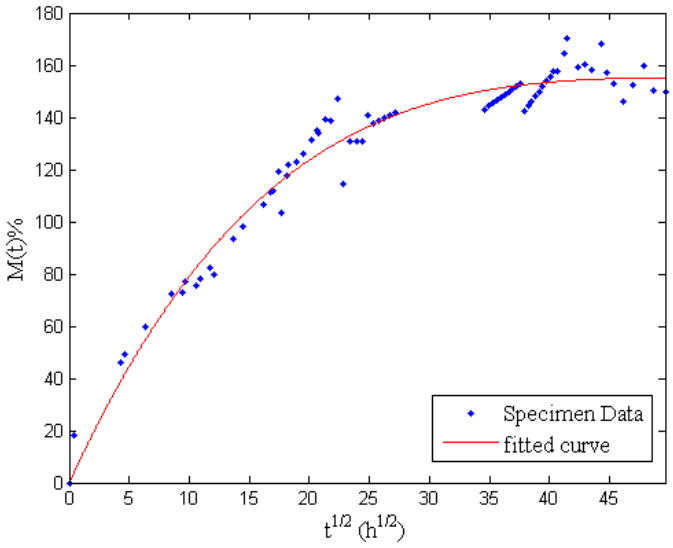

Figure 2.2: Moisture uptake of specimens exposed to synthetic sea water

2.3.2 Effects of Sea Water Uptake on Compressive Response

Specimens were subjected to compressive loading at room temperature upon reaching sea water uptake equilibrium, which corresponds to SNR. Four samples were tested for each type of test condition, while the fifth sample was retained to examine surface degradation and the amount of water diffusion in the sample. Sea water saturated samples tested under room temperature conditions manifested a decrease in compressive strength by ≈12.1% and a decrease in compressive modulus by 9.87% with respect to dry samples. Similar decrease in modulus was also observed in low density polyvinyl chloride foams as reported by earlier researchers [21]. Table 2.3 summarizes the experimentally obtained values of compressive

stiffness and strength for saturated and dry samples.

Table 2.3: Mechanical properties of conditioned samples

Conditioning	Comp. Strength (MPa)	Comp. Modulus of Elasticity (MPa)
Dry	0.686±0.049	12.323±1.019
Sea Water	0.603±0.012	11.107±0.383

Degradation in the mechanical properties of samples conditioned with synthetic sea water can be attributed to their surface deterioration, as shown in Figure 2.3. The presence of water is evident in the conditioned samples where the cell walls are blurred as a result of water uptake. Surface deterioration of the samples enhanced the filtration of fluid into the material, thereby, increasing the moisture content and consequently decreasing their mechanical properties [22].

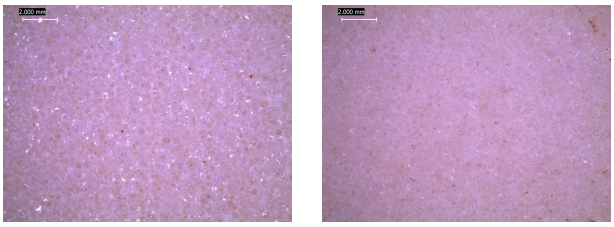

(a) (b)

Figure 2.3: Dry sample with no conditioning compared to the degraded surface of a synthetic sea water saturated sample: (a) Dry sample surface; (b) Synthetic sea water saturated sample surface

One of the untested saturated samples was cut through its cross-section to examine the extent of the water diffusion into the material. The images obtained using a stereoscope (LEICA M205 C) showed that the penetration of synthetic sea water in the specimens ranged between 2-3 mm from the exposed surfaces. The sea water absorption was limited only to the boundary region of the sample, which corroborates a lower influence on the reduction of compressive strength and modulus properties. The extent of sea water infiltration into the material and the overall degradation is shown in Figure 2.4.

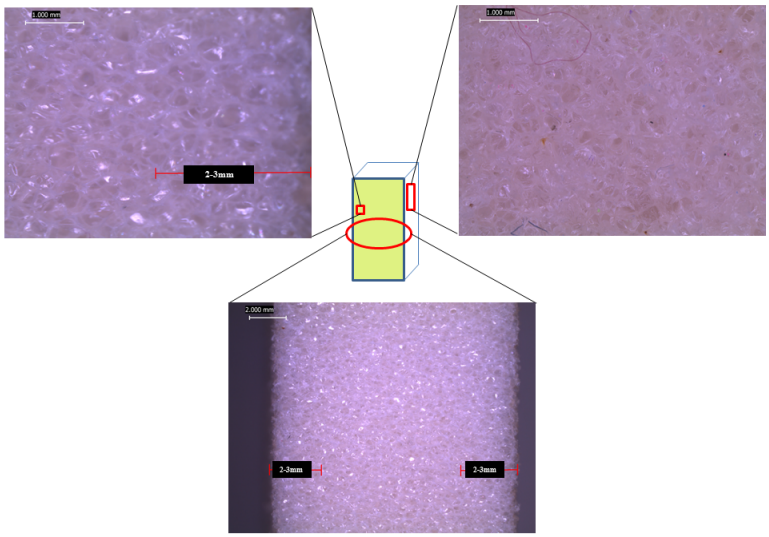

Figure 2.4: Schematic of Cross-Section of Sea Water Exposed Sample.

2.3.3 Effects of Arctic Exposure on Compressive Behavior

Arctic tests were divided into three main categories: dry arctic, semi-saturated arctic, and saturated arctic exposed samples. For each of these three categories, tests were performed at room temperature (23^{o}C) and at arctic conditions (-60^{o}C) in order to investigate the compressive properties of the material. The procedure followed for these tests were the same as that of saturated samples with the addition of the environmental chamber for in-situ arctic conditions. Given that the moisture content at saturation was previously calculated, semi-saturated samples were first exposed to synthetic sea water until the moisture content in the samples reached approximately half the value of M_{sat} discussed above. These samples were exposed to arctic condition (-60^{o}C) for a period of 48 hours before conducting compression tests. Same procedure was followed for completely saturated samples. A representative graph of one compression test under each condition considered in this study is shown in Figure 2.5. All the responses are compared against the blue solid response, which corresponds to DNR.

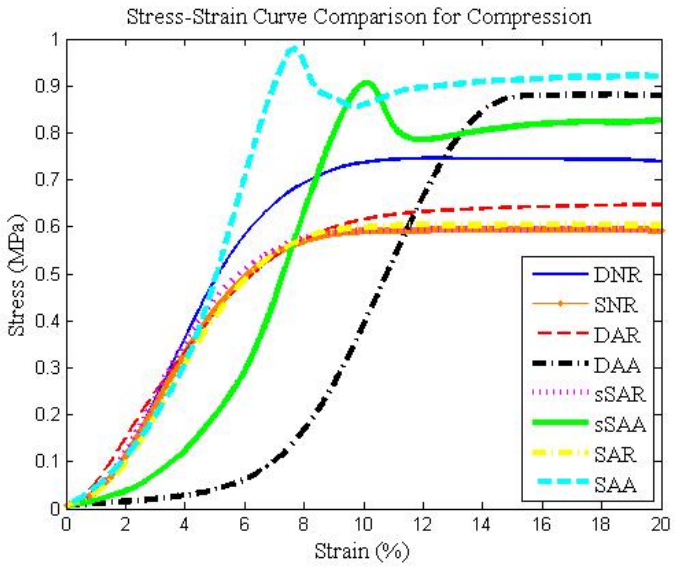

Figure 2.5: Compressive Stress-Strain response for dry and arctic exposed samples.

In Figure 2.5, all the responses have similar overall trend in the stress-strain response with a linear-elastic region at the beginning followed by a plateau, known as stress plateau [3]. The value of stress corresponding to the plateau region was considered to be the maximum strength of the samples here, since they did not display significant increase or decrease in stress. Upon further loading the samples, the stresses continue to increase due to the densification of material. Aside from this behavior, no typical failure point was observed during or after the plateau region in the compressive stress-strain response. The compressive properties obtained for each type of exposure and testing condition from all tests conducted are summarized in Table 2.4 and shown in Fig. 2.6. The percentage change in compressive modulus and strength are determined with DNR as the baseline condition.

Table 2.4: Mechanical properties of arctic conditioned samples

Conditioning	Compressive Strength(MPa)	% Change w.r.t DNR	Compressive Modulus of Elasticity(MPa)	% Change w.r.t DNR
DNR	0.686±0.049	—	12.323±1.019	—
SNR	0.603±0.012	-12.1	11.107±0.383	-9.87
DAR	0.641±0.011	-6.48	11.151±0.058	-9.51
DAA	0.857±0.021	25.03	11.669±1.593	-5.31
sSAR	0.608±0.007	-11.32	11.752±0.112	-4.63
sSAA	0.908±0.044	32.39	18.140±1.616	47.02
SAR	0.611±0.008	-10.94	10.809±0.505	-12.29
SAA	0.995±0.031	45.06	21.225±0.773	72.23

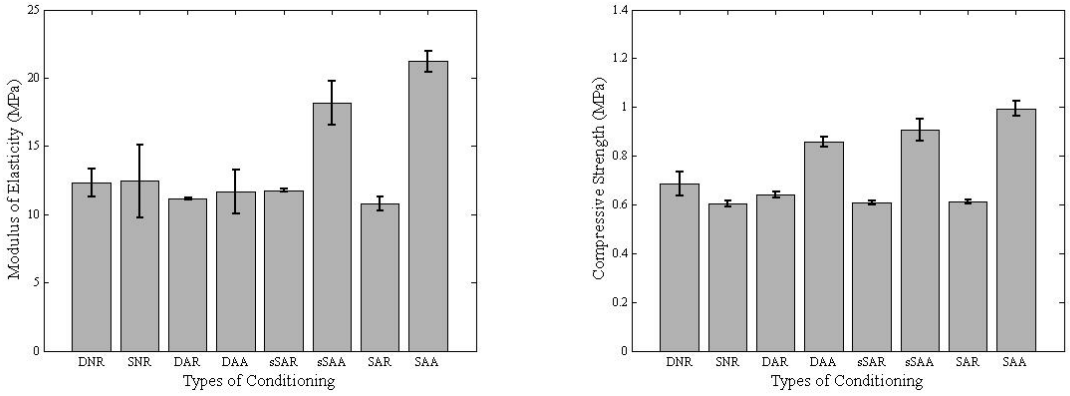

Figure 2.6: Variation in (a)compressive modulus and (b)compressive strength with respect to the type of conditioning.

It is observed from Fig. 2.6 that the compressive strength typically increases when the samples are tested in-situ arctic (-60°C) temperature, which is attributed to the rigidity imparted by freezing temperature and solidification of any water present in saturated and semi-saturated samples. Hence, the maximum increase in compressive strength was observed in saturated samples tested in in-situ arctic condition (SAA). The compressive strength decreased under all other exposures, specifically a significant reduction is observed

in the samples saturated (or semi-saturated) with sea water and exposed to arctic temperatures which are then subjected to compression at room temperature (SAR or sSAR). This condition represents a thawed saturated foam subjected to compression at room temperature. This is corroborated by the micrographs of the tested samples shown in Fig. 2.7. Maximum deformation and internal damage is observed in the cases corresponding to sSAR and SAR as shown in Fig. 2.7 (e) and (g).

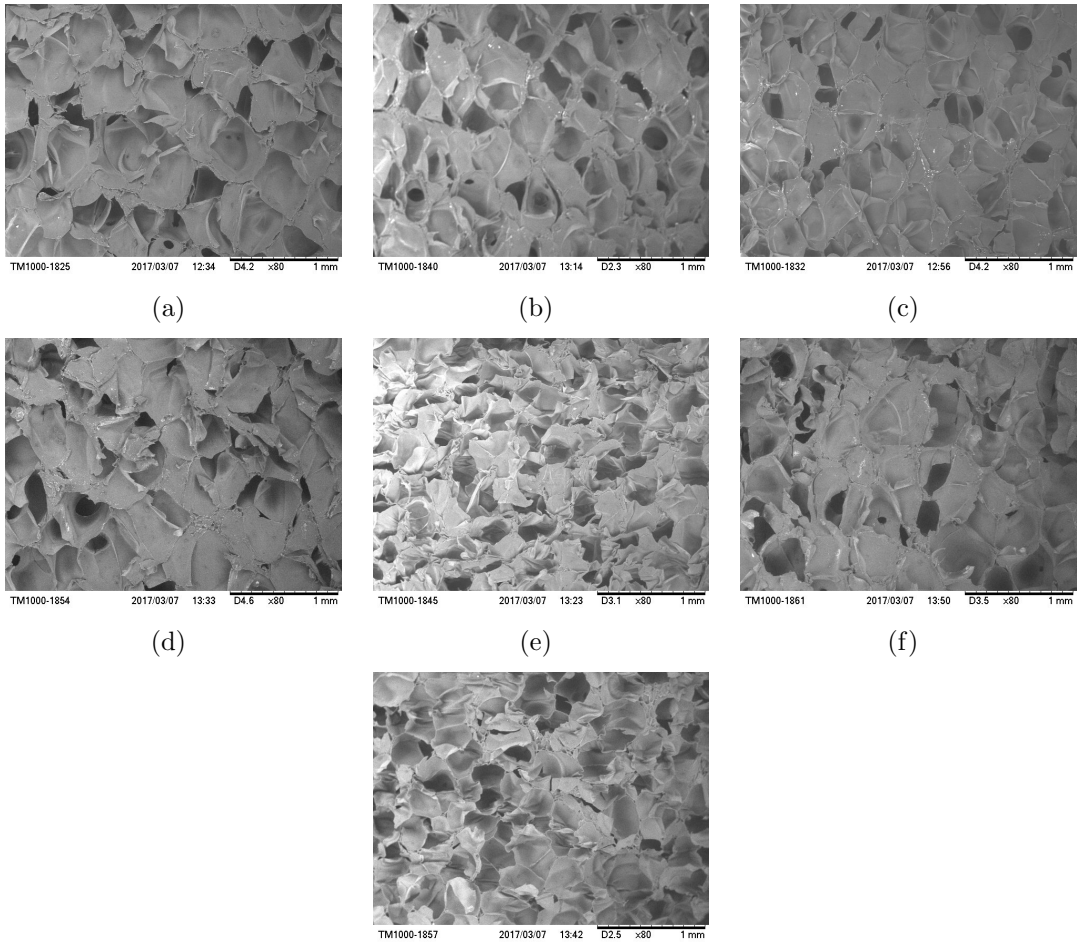

Figure 2.7: Micrographs of the cross-section of exposed specimen after testing for (a)DNR, (b)DAA, (c)DAR, (d)sSAA, (e)sSAR, (f)SAA, and (g)SAR.

To elaborate further, it was observed that in-situ room temperature testing after arctic

conditioning had the maximum adverse effect on PVC foams. That is, XAR samples manifested inferior mechanical properties than XAA samples. For example, in the case of wet specimens (SAR or sSAR) subjected to arctic conditioning and tested at in-situ room temperature, the decrease in their strength and moduli can be attributed to the internal damage caused by drastic change in temperature, in addition to the surface degradation caused by the sea water that was absorbed by the samples. These samples experienced drastic change in temperature when they were exposed from room temperature(23^oC) to arctic conditions (-60^oC) and then back to room temperature (23^oC) for testing. In contrast, sSAA and SAA samples manifested an increase in their properties due to the rigidity experienced by the foam as well as freezing of sea water absorbed due to arctic exposure and in-situ arctic testing. That is, the samples became less compliant during compression under in-situ arctic environment, thereby increasing their strength. From this study, it can be concluded that the samples conditioned with sea water and exposed to arctic temperature for a short period of 48 hours can result in significant reduction in compressive properties at room temperature.

2.4 Conclusion

In this paper, the influence of sea water arctic exposure on the compressive properties of PVC foams was examined. Eight different cases were considered: 1) Dry conditioning + in-situ room temperature testing - DNR; 2) Dry + arctic conditioning + in-situ room temperature testing - DAR; 3) Dry + arctic conditioning + in-situ arctic testing - DAA; 4) semi-Saturated + arctic conditioning + in-situ room temperature testing - sSAR; 5) semi-Saturated + arctic conditioning + in-situ arctic testing - sSAA; 6) Saturated conditioning + in-situ room temperature testing - SNR; 7) Saturated + arctic conditioning + in-situ room temperature testing - SAR; 8) Saturated + arctic conditioning + in-situ arctic testing - SAA. Key observations from these eight cases were:

1. Room temperature compressive properties in general appear to decrease in condi-

tioned foams, but increased at -60^{o}C. This is attributed to the rigidity imparted to the samples due to freezing at arctic temperatures.

2. Room temperature compressive strength and modulus of arctic conditioned foams (DAR) decreased by about 7% and 10%, respectively, which is attributed to the freeze-thaw effect.

3. Under sea water conditioning, it was observed that the water absorption was confined to a thin region in the exterior of the samples only. In the case of only arctic exposed samples, surface damage or degradation was not apparent.

4. Saturated samples tested at in-situ room temperature (SNR) appear to reduce the compressive strength and modulus by approximately 12% and 10%, respectively. Such response it related to the the surface degradation of foams due to sea water saturation.

5. Room temperature compressive properties of sea water saturated foams conditioned further at -60^{o}C for 48 hours (SAR) reduced by 11% and 13% in strength and modulus, respectively. The influence of freeze thaw in addition to the degradation due to sea water saturation has the maximum adverse effect.

6. In contrast, saturated and semi-saturated arctic exposed samples tested at -60^{o}C (SAA and aSAA) manifested significantly higher strength and modulus as compared to the baseline condition, due to the combined effect of rigidity imparted to the foam and freezing of the absorbed sea water.

In conclusion, long term sea water conditioning along with arctic exposure is detrimental to the mechanical properties of PVC foams. By exposing the foams directly to sea water environment, this study shows the worst case scenario for foam cores used in sandwich composites, since the foam core material is not in direct contact with the environment. In sandwich construction, the foam cores are sandwiched between thin laminates. However, it is important to investigate the response of foam core materials under these types of

environments to prevent any premature failure of the interfaces between foam core and face sheet laminates in sandwich composites.

Chapter 3

Compressive Behavior of Cenosphere/Epoxy Syntactic Foams in Arctic Conditions

3.1 Introduction

Sandwich composites have gained significant importance in recent years from context of replacing conventional engineering materials for naval applications due to favorable properties such as lightweight and the ability to tailor mechanical properties. These sandwich composites typically consist of a lightweight core which is sandwiched between two fiber-reinforced laminated facesheets in order to provide the basis for a strong and stiff structure. Closed-cell low-density polymeric foams are targeted for naval crafts as they are ideal for such applications. Naval structural materials are typically exposed to critical conditions for extended periods of time, which can be detrimental to the mechanical properties. Few commonly experienced conditions are exposure to sea water, temperature changes in the water, wave impact, etc. Further, with increased interest in arctic exploration, these materials could be exposed to harsh conditions of the arctic region. Therefore, it is of utmost importance to understand how such material behave under these extreme conditions. The focus of the present work is on exploring the behavior of a foam core material, called syntactic foams, under arctic exposures.

Syntactic foams are closed cell composite foams, which consist of hollow microspheres dispersed in a matrix resin [23]. Given the advantage of syntactic foams over other materials due to their tailor made properties [23, 24], these foams have been employed in distinct engineering applications such as structures like ribs, hulls and decks of ships for marine exploration. Previous researchers have investigated the behavior of syntactic foams with engineering glass microballons as the filler material [25, 26]. Sodalime-borosilicate glass is a major constituent of these engineered glass particles. However, it has been shown that

the degradation of such syntactic foams is due to dealkalization of glass [27]. In the present study, cenospheres are used as filler material in the foams. These are hollow particles of fly ash, which is an industrial waste material and a potential environmental pollutant. Fly ash is a by-product of coal plants and are primarily comprised of alumina and silica. Use of cenospheres in syntactic foams can help the environment by minimizing waste, while creating foams with better properties [28, 29, 30, 31].

Extensive studies have been performed in the past for understanding the behavior of syntactic foams in order to be able to tailor their properties accordingly for a wide range of applications [32, 33, 34, 35, 25]. For example, in the work presented by Gupta, Woldesenbet, and Mensah [36], it was shown that the compressive strength and modulus of syntactic foams increased with reducing internal radius of cenospheres while keeping all other parameters the same. The relationship that exists between the fillers and matrix is rather complex and can pose issues when trying to modify the mechanical properties of syntactic foams. Therefore, different types of tests have been performed on syntactic foams, such as three-point bending tests in either flexural [37, 38, 39, 40] or short beam shear tests[41, 42, 43] in order to determine their response under these types of loading. Also, other studies have been performed for capturing the response of syntactic foams under compressive [44, 45, 46, 47, 48, 49], hygrothermal [50, 51, 52], and impact loading [53]. In many of these studies, only the effect of varying the filler content on the mechanical properties is reported. Other aspects such as particle wall thickness variations, interfacial bonding, and the porosity of the walls of the hollow spheres in cenosphere/epoxy foams makes it challenging to establish structure-property correlations. Furthermore, studies have been performed in order to help reduce the time and effort that it take to characterize the material behavior. In works presented by Zeltmann et al. [54, 55], methods to predict strain rate sensitivity in the modulus of polymers and polymer matrix composites was developed using dynamic mechanical analysis data. The methods allowed to obtain the modulus of the specimen for various strain rates.

In many experimental investigations, it was observed that the mechanical properties are

affected by water absorption by the syntactic foams [39, 50, 52, 56]. A majority of these studies along with previously mentioned studies were carried out under room temperature conditions. In the case of marine vessels for Arctic or Antarctic exploration, understanding the behavior of syntactic foams at subzero temperatures is very important. Nevertheless, there is no literature that discusses the effect of arctic environment on the compressive properties of cenosphere/epoxy foams. The present study explores this case by investigating the change in compressive properties of syntactic foams due to change in external temperatures. Cenosphere material, matrix resin, surface modification of filler and volume fractions are maintained between syntactic foams at room and arctic temperatures. Changes in the compressive response, failure and fracture patterns can be attributed to the operating temperature. The novelty of the present study include: (a) use of industrial waste fly ash cenospheres for developing eco-friendly syntactic foams and (b) structure-property correlations under arctic conditions.

This paper is organized in the following sections: Section 3.2 presents a description of the material constituents, manufacturing process of the samples, the process to expose the samples to arctic environment and the procedure for compressive testing. This is followed by Section 3.3, where the results from material processing and compression tests with and without arctic exposure of cenosphere/epoxy foams are presented. Finally the conclusions of this study are reported.

3.2 Materials and Methods

3.2.1 Constituents

Fly ash cenospheres of CIL 150 grade used as filler in this study are procured from Cenosphere India Ltd., Kolkata, West Bengal, India. Table 4.1 presents the details of the chemical, physical and sieve analysis in as received condition. Cenospheres primarily comprise of alumina, silica, calcium and iron oxides as observed from this table. Lapox L-12 epoxy resin with K-6 hardener, supplied by Atul, Valsad, Gujarat, India is the matrix resin used. Syntactic foams are prepared with two configurations: 1) with as received ceno-

spheres and 2) surface modified cenospheres. Silane coating on cenospheres is carried out using 3-Amino propyl tri ethoxy silane (APTS), procured from Sigma Aldrich, Bangalore, India. A minimum of five specimens are tested in compression under room temperature and arctic conditions.

Table 3.1: Chemical, physical and sieve analysis details of cenospheres

Physical properties	Chemical analysis	Sieve analysis			
True particle density	920 kg/m^3	SiO_2	52-62%	+ 30 # (500μm)	Nil
Bulk density	400-450 kg/m^3	Al_20_3	32-36%	+ 60 # (250μm)	Nil
Hardness (MOH)	5-6	CaO	0.1-0.5%	+100 # (150μm)	Nil
Compressive strength	180-280 kg/m^3	Fe_20_3	1-3%	+150 # (106μm)	0-6%
Shape	Spherical	TiO_2	0.8-1.3%	+ 240 # (63μm)	70-95%
Packing factor	60-65%	MgO	1-2.5%	- 240 #	0-30%
Wall thickness	5-10% of shell dia.	Na_2O	0.2-0.6%		
Color	Light grey - light buff	K_2O	1.2-3.2%		
Melting point	1200 - 1300 ^{o}C	CO_2	70%		
pH in water	6-7	N_2	30%		
Moisture	0.5% max.				
Loss on ignition	2% max.				
Sinkers	5% max.				
Oil absorption	16 - 18 g/100 g				

[1]As specified by supplier

3.2.2 Surface modification of cenospheres

In syntactic foams, the volume fraction and size of cenospheres can alter the overall mechanical properties. Apart from the volume fraction and size, the interaction between cenospheres and epoxy plays a major role in load transfer mechanism between the constituents [57]. The mechanical properties of cenosphere reinforced polymer composites are inferior owing to poor interfacial interactions between the hydrophilic cenosphere surface and hydrophobic polymer. Silane coupling agents are usually used as adhesion promoters between inorganic filler and organic matrix. In the present study, cenospheres are surface treated with silane by mixing 50 g of cenospheres into 100 ml solution of water/ethanol (20:80 wt. %). Further, 2% by volume of APTS is added into the solution and continuously stirred for 30 minutes at 80^{o}C in a microwave reactor (Enerzi microwave systems,

Bangalore, India). The resultant product is filtered, washed at least three times using a mix of water/ethanol and then dried in an oven to extract the coated cenospheres.

3.2.3 FTIR, XRD and Particle size analysis

Cenospheres are analyzed by FTIR spectroscopy (JASCO 4200, Japan, Automated Total Reflection mode, wave number 4000 to 650 cm^{-1}) to confirm the silane coating. X-ray diffractograms are determined for 2θ values using DX GE-2P, JEOL, Japan having Nickel filter material with scanning speed of 2^o/min and Cu Kα (λ=1.514 A^o) radiation. Particle size and shape analysis is conducted using a Sympatec (Pennington, NJ) QICPIC high speed image analysis system [58, 59].

3.2.4 Sample preparation

Syntactic foams are fabricated by mixing desired volume fraction of cenospheres with Lapox L-12 epoxy resin and K-6 hardener at room temperature. The mixture is gently stirred to obtain a homogeneous and uniform slurry, followed by adding 10 wt.% hardener and finally degassing the mixture for 4 min prior to casting in aluminum molds. The cast slabs are cured at room temperature for 24 hours and post cured at 90^oC for 3 hours. Three different syntactic foams with varying cenosphere volume fraction of 20, 40 and 60 vol. % in epoxy matrix are fabricated. This procedure is adopted for both as received and silane treated cenospheres. Additionally, neat resin specimens, i.e., without any filler in the matrix, are also fabricated for comparision. Samples are named according to the convention EXX-Y, where E denotes epoxy resin, XX is the volume fraction of cenospheres and Y represents filler modification condition (U denotes untreated and T represents treated cenospheres). Cast slabs are trimmed using diamond saw cutter to confirm the dimensions as mentioned in ASTM D695 (compression). The densities of all the samples are measured using the procedure as outlined in ASTM D792-08. Theoretical density is computed using rule of mixture and is given by,

$$\rho_c = \rho_f V_f + \rho_m V_m \tag{3.1}$$

where, ρ and V are density and volume fraction, respectively. Subscripts c, f and m denote composite, filler and matrix, respectively. Furthermore, the void content (Φ_v) is estimated using theoretical (ρ^{th}) and experimental (ρ^{exp}) densities and is given by [36, 38],

$$\Phi_v = \frac{\rho^{th} - \rho^{exp}}{\rho^{th}} \tag{3.2}$$

3.2.5 Arctic conditioning

To the knowledge of the authors, there is no standard for arctic exposure studies. Therefore, a procedure for specimen conditioning is developed in-house, which is similar to the initial conditioning for water intake measurements as mentioned in ASTM C272 and D5229 standards. Prior to any type of conditioning and testing, the syntactic foams are oven dried for 24 hours to eliminate moisture content absorbed during processing, if any. Further, five samples for each volume fraction for both untreated and treated categories are placed in a freezer, which is maintained at -60^{o}C. All specimens are then conditioned for 57 days, after which the specimens are mechanically tested under in-situ arctic conditions (-60^{o}C). The procedure followed to obtain the mechanical properties for the syntactic foam samples is discussed in the following section.

3.2.6 Compression tests

All the specimens are mechanically tested in compression at room (30^{o}C) and arctic temperatures (-60^{o}C) using Instron 5969 Tabletop Universal Testing system. A crosshead displacement rate of 1.3 mm/min is applied on 12.7 mm x 12.7 mm face of each specimen following the ASTM D695 standard. Compressive modulus and ultimate strength are calculated using the following equations:

$$E_z^c = \frac{(P_{0.00x2} - P_{0.00x1})h}{(\delta_{0.00x2} - \delta_{0.00x1})A}; \qquad F_z^c = \frac{P_{max}}{A} \tag{3.3}$$

where, E_z^c is the compressive modulus, $P_{0.00x}$ is the applied force at a given deflection, h is the specimen mean height, $\delta_{0.00x}$ is the recorded deflection value, A is the cross-sectional area, F_z^c is the ultimate compressive strength, and P_{max} is the ultimate force prior to failure.

3.3 Results and Discussions

3.3.1 Fabrication and Material processing

Fly ash cenospheres used in the present study are used in as received (untreated) and silane modified (treated) conditions. FTIR results for untreated and silane treated cenospheres are presented in Figure 3.1a. The spectrum confirms the presence of a silane surface layer and the C-H stretching of propyl group is observed at 2929 cm^{-1}. XRD diffraction results of as received and silane modified cenospheres is exhibited by Figure 3.1b. Untreated and treated fly ash cenospheres has a main peak at 2θ value of 26.6 and 26.04 and other numerous small peaks manifesting mainly metal oxides, predominantly SiO_2 and $3Al_2O_3$, respectively.

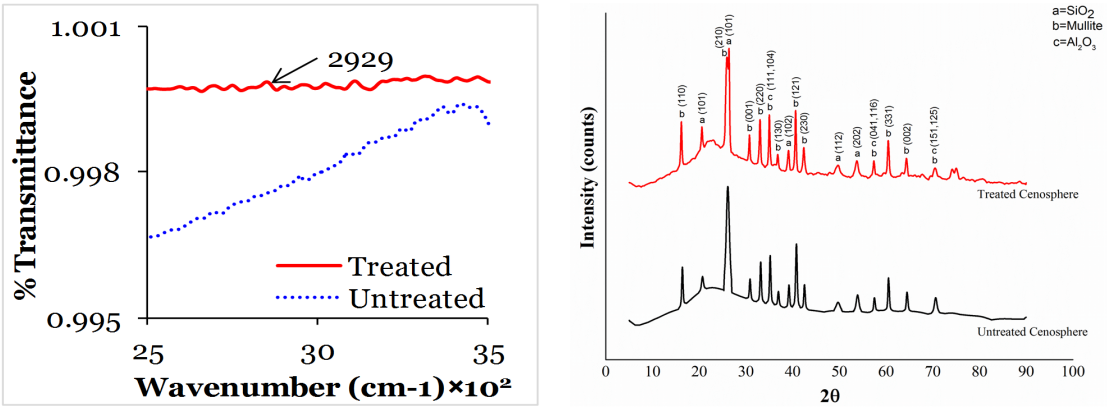

(a) (b)

Figure 3.1: (a) A section of the FTIR spectra of untreated and silane treated cenospheres; (b) X-ray difftractogram of cenospheres.

Figure 3.2 presents micrographs of untreated and treated cenospheres, respectively. The coating layer is not visibly identifiable in the micrographs due to its small thickness, despite,

FTIR results confirm the silane presence on cenospheres. Surface morphology is not uniform for fly ash cenospheres due to variations in sphericity and presence of numerous defects as seen from these micrographs. One such broken cenospheres is micrographed at higher magnification, and is shown by Figure 3.2c. Porosity in the cenosphere walls and irregular wall thickness is clearly evident from the micrograph, which might lead to lower mechanical properties as compared to non-porous ones. Such variations may lead to deviation of the experimental investigation from that predicted by empirical and/or mathematical models.

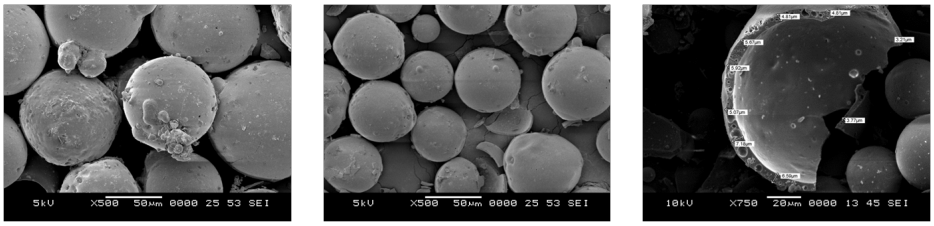

(a) (b) (c)

Figure 3.2: Cenosphere micrographs of (a) untreated (b) treated and (c) one such broken treated particle. Wall thickness variations and built-in porosity in fly ash cenospheres are clearly evident from the micrograph.

Untreated and treated cenospheres are subjected to particle size analysis and the results are presented in Figure 3.3. It can be observed that the volume weighted mean particle size for untreated and treated particles are 99.5 and 110.2 μm, respectively. Broader peak is seen in the case of treated particles. Untreated and treated cenospheres registered X50 median particle sizes of 76.3 and 98.1 μm, respectively, confirming an increase in average diameter owing to silane treatment. Densities of as received and treated cenospheres are measured to be 0.92 and 1.0 kg/m^3. Sphericity of cenospheres is observed to be in the range of 0.6-0.85 [58]. Deviation from 1, a perfectly spherical particle, might be due to surface defects as observed in Figure 3.2a. Shift in the curve of treated particles in the plot can also be attributed to particle coating. From Figure 3.3, considerable extension is seen at the tail end of the curve for the treated particle indicating a small amount of cluster formation. Shear forces induced during manual stirring is expected to disperse some of

these clusters formed, if any.

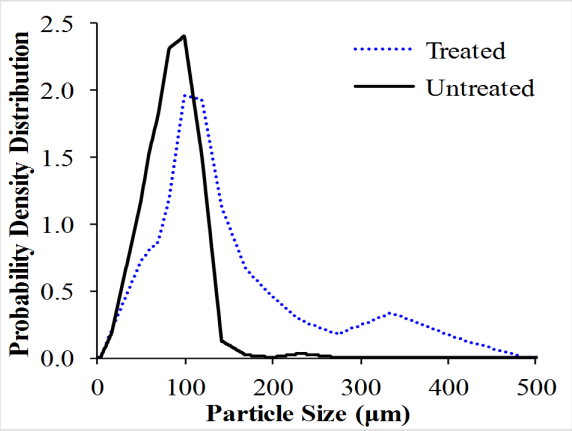

Figure 3.3: Particle size analysis of untreated and treated cenospheres.

Synthesizing syntactic foam composites with uniform dispersion of cenospheres, minimum cluster formation and particle failure in the matrix during processing is a challenging task. Manual stirring is used in the present work to prepare cenosphere/epoxy foams. Micrographs of as cast cenospheres/epoxy foams are presented in Figure 3.4. Uniform dispersion of hollow cenospheres, both untreated and treated, in the matrix is observed in Figure 3.4a-b demonstrating the feasibility of using manual stirring for developing such syntactic foam composites. Further, clusters are not observed to be formed in the foams with treated cenospheres (Figure 3.4b) as anticipated from Figure 3.3. Clusters are expected to be broken effectively due to shear forces induced due to stirring of the cenospheres/epoxy slurry. Interfacial adhesion between the epoxy resin and the as received cenospheres appears to be poor as seen in Figure 3.4c. Silane modification of cenospheres shows good adhesion between the constituents as seen from Figure 3.4d. Improvement in the interfacial bonding is expected to improve the load transfer from the matrix to the particle and improve the overall properties of syntactic foams. Load transfer between filler and the matrix along with failure mechanisms are governed by interface topology. Flexural and tensile properties are strongly affected by the interfacial bonding strength [58, 59, 60, 61] as interfacial cracks tend to form under such conditions. However in compression, the mechanical properties

are less sensitive to interfacial adhesion [62, 63]. Nevertheless, non-uniform layer of coating makes comparison of mechanical properties very challenging [38], and is beyond the scope of the present work.

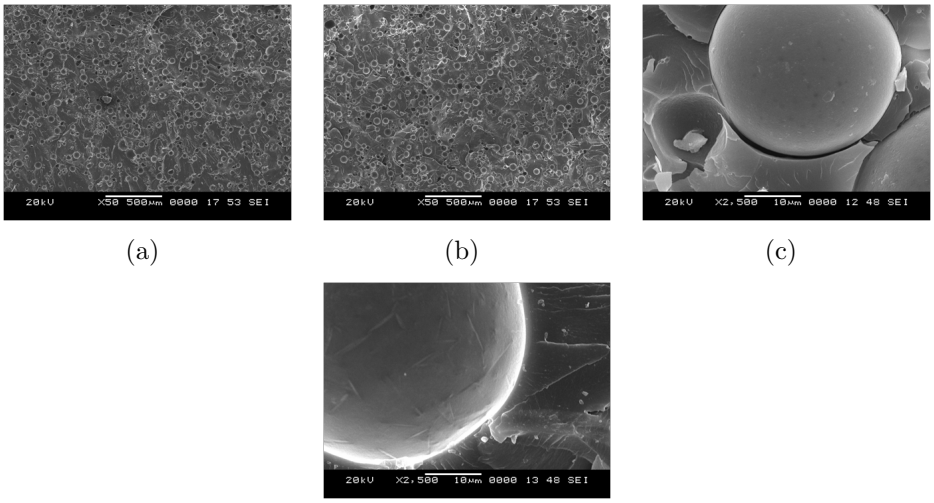

(a) (b) (c)

(d)

Figure 3.4: Micrograph of as cast (a) E20-U (b) E20-T foams showing uniform dispersion of cenospheres. Lack of bonding between for E20-U is seen in (c) while good interfacial bonding is evident from (d) due to silane treatement in E20-T.

Quality and the mechanical properties of syntactic foam samples depend on the survival of the hollow cenospheres and the void content due to entrapped air during processing. Therefore, it is necessary to quantify and correlate these parameters with the properties being investigated. Table 4.2 presents the density and void content estimations. Theoretical densities are computed using Eq. 4.1, which are higher compared to the experimental ones as seen from Table 4.2. Reduction in the density of composites determined experimentally as compared to the theoretical ones is attributed to the air entrapment in matrix during the process of mechanical mixing of cenospheres in the resin. The presence of very few entrapped air pockets are observed in Figure 3.2, which are characteristic of typical syntactic foams. Such entrapped air is undesired as it adversely affects the mechanical properties and is referred to as voids. The void content was calculated using Eq. 4.2.

Table 3.2: Density and Void volume fraction of syntactic foams.

Material	ρ^{th} (kg/m^3)	ρ^{exp} (kg/m^3)	ϕ_v (%)	Weight saving (%)
E	—	1.1920 $\pm 0.410^{-3}$	0.34	—
E20-U	1.1376	1.1296 $\pm 0.910^{-3}$	0.70	9.06
E40-U	1.0832	1.0647 $\pm 1.210^{-3}$	1.71	11.45
E60-U	1.0288	1.0283 $\pm 1.810^{-3}$	0.05	16.12
E20-T	1.1536	1.1331 $\pm 1.210^{-3}$	1.78	5.09
E40-T	1.1152	1.0739 $\pm 2.110^{-3}$	3.70	8.78
E60-T	1.0768	1.0556 $\pm 3.510^{-3}$	1.98	11.91

As seen from Table 4.2, the void content appears to increase with increase in filler content. The presence of such voids further reduces the matrix content. The amount of matrix present at 60 vol. % filler loading is much lesser compared to other compositions resulting in much lower void content. Density of foams with treated cenospheres registered higher density values for all the compositions prepared. Silane coating on as received cenospheres increases the effective mean diameter, thereby increasing their density. Narrow variations in standard deviations are observed affirming consistency in specimen processing. Further, weight saving potential is estimated as compared to neat epoxy samples, and values are listed in Table 4.2. Lower densities of syntactic foams with untreated cenospheres noted to have better weight saving. Specific mechanical properties are worth investigating for exploiting these lightweight cenosphere/epoxy foams in Naval applications. It would be an interesting task to understand and analyze the effect of arctic environment on such abundantly available untreated/treated hollow fly ash cenospheres to propose suitable applications.

3.3.2 Compressive modulus and strength

Figure 3.5 presents representative compressive stress-strain curves for all types of cenosphere/epoxy syntactic foams investigated. The unconditioned (dry) neat resin and the syntactic foams show similar stress-strain profiles until peak stress, which consists of a linear elastic region followed by a strain softening that is characterized by a drop in stress

carrying capacity. Upon further loading the specimens in compression, the stress starts rising again in neat epoxy samples up to around 15% strain value after which it starts to drop until final fracture. The post peak increase in stress is faster and significantly higher in the case of neat resin, whereas for syntactic foams it depends on the volume fraction and surface modification of hollow fillers. In both treated and untreated syntactic foams, the strain at final fracture decreases with increasing percentage of cenosphere volume fraction.

For the case of arctic exposed samples, both treated and untreated cenospheres/epoxy foams demonstrated a brittle behavior. Upon reaching a maximum load carrying capacity, a slight decrease in stress is observed before complete failure of the samples. The compression rate is held constant in this experimental study at the ASTM standard recommended value, as the stress-strain behavior can potentially be a strain rate dependent phenomena [64, 65]. In Figure 3.5, it can be noted that all syntactic foam compositions do not show a stress plateau, which is seen as a typical feature for most types of syntactic foams, including epoxy and aluminum matrix syntactic foams [66, 67].

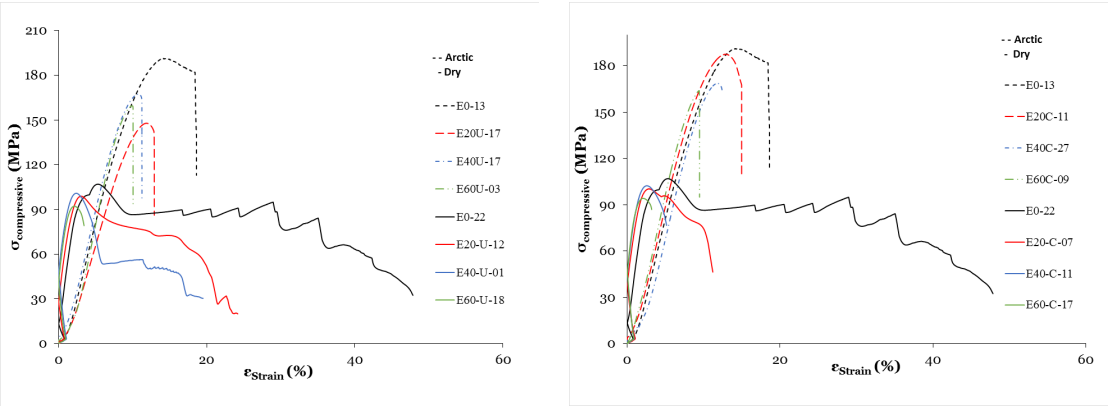

(a) (b)

Figure 3.5: Representative stress-strain curves obtained in compressive testing of syntactic foams containing 20, 40 and 60 by volume % (a) untreated and (b) treated cenospheres.

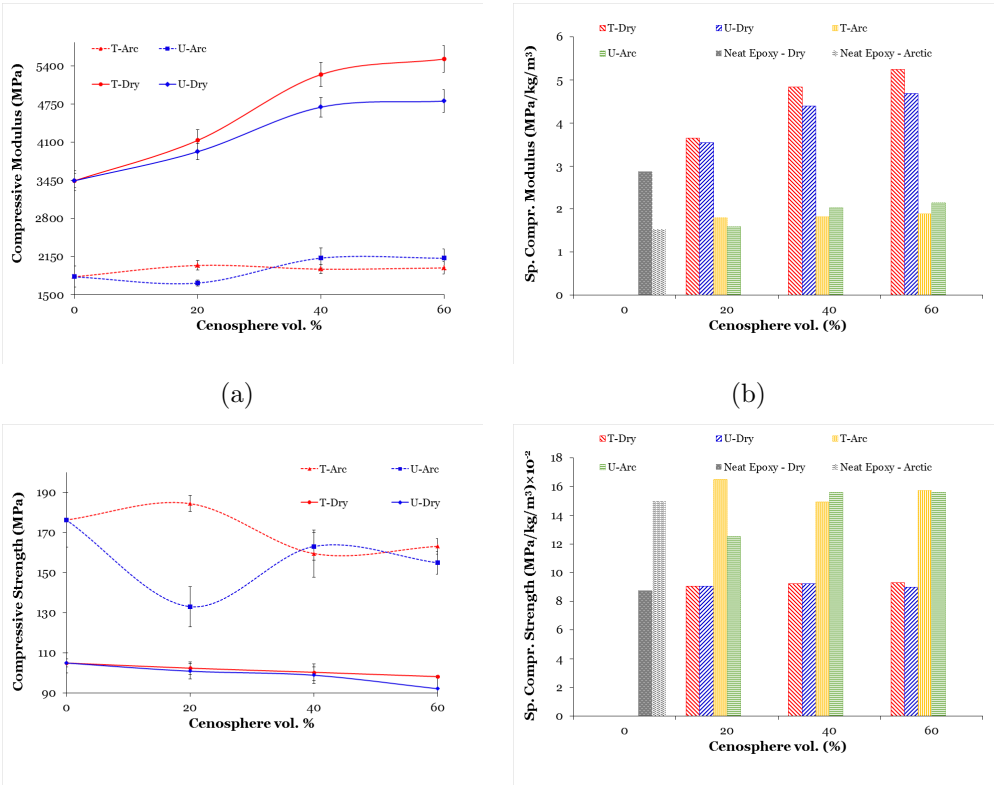

Figure 3.6: Experimentally measured compressive (a) modulus (b) specific modulus (c) strength and (d) specific strength of syntactic foams.

Compressive modulus is determined as the slope of the initial linear region of the stress-strain responses and are presented in Figure 3.6a-b. It is observed that the compressive modulus increases with increase in cenosphere content, for both untreated and treated fillers. Significant rise is observed for EXX-T foams with higher filler content. Also, the compressive modulus values are significantly higher in syntactic foams as compared to that of the neat resin. Further, the specific moduli (modulus divided by the foam density) for EXX-T composites are 26-81% higher than the neat resin as exhibited in Figure 3.6b. Significant advantage over the neat resin in terms of weight saving can be achieved if EXX-T foams are used in compressive loading conditions. Compressive strength is defined as the first peak in the stress-strain response. Figure 3.6c-d shows the compressive strength values,

Table 3.3: Compressive Modulus and Strength properties of syntactic foams.

Material	Compressive(MPa)			
	30^{o}C		-60^{o}C	
	Modulus	Strength	Modulus	Strength
E	3443.46 ±119.78	104.88 ±2.01	1807.48 ±179.13	176.26 ±13.57
E20-U	3939.28 ±137.03	100.79 ±3.79	1701.09 ±50.92	133.01 ±9.98
E40-U	4697.47 ±165.68	98.79 ±4.1	2125.45 ±171.09	163.03 ±6.96
E60-U	4800.71 ±197.21	92.06 ±5.53	2124.40 ±156.44	154.87 ±5.67
E20-T	4132.08 ±179.78	102.29 ±3.14	2001.20 ±80.54	184.41 ±4.01
E40-T	5253.51 ±206.85	100.26 ±4.03	1937.16 ±76.13	159.48 ±11.82
E60-T	5518.09 ±231.88	98.11 ±0.62	1959.14 ±107.00	163.10 ±3.91

where it is observed that an increase in cenosphere volume fraction in both EXX-U and EXX-T configurations decreases the compressive strength value. Compressive strength values of all the foams tested are lower compared to neat epoxy samples. Nevertheless, results for specific compressive strengths (compressive strength divided by the density) for all the foam compositions are comparable or marginally higher than that of the neat resin.

For the arctic conditioned samples, both treated and untreated cenosphere/epoxy foams manifest a brittle behavior in their stress-strain responses. By comparing the arctic conditioned samples to the unconditioned (dry) samples, a decrease in compressive modulus of elasticity by 47-57% and 47-65% is observed for untreated and treated cenospheres/epoxy syntactic foams, as shown in Table 4.3. On the other hand, the compressive strength values increased by a range between 32-68% for untreated cenospheres and 59-80% for treated cenospheres in in-situ arctic samples. The arctic conditioning appears to have degraded the foams causing a reduction in the the compressive modulus. However, in-situ arctic condition introduced rigidity to the material during the compression tests causing an increase in the compressive strength values.

Fracture features of neat epoxy and syntactic foams with two volume fractions of cenospheres are compared in Figure 3.7. Prominent shear crack and excessive plastic deforma-

tion marks are observed in neat epoxy sample (Figure 3.7a). Syntactic foams containing 20 vol.% cenospheres deform with fewer cracks than those containing 60 vol.% ones for EXX-U and EXX-T configurations. The failure features of these specimens are similar to those observed in the work presented by Gupta [44]. Shear cracks form and propagate with fragment formation from the sidewalls. Brittleness of the foams increases at higher filler percentages due to the inclusion of relatively brittle cenospheres in ductile matrix. At E60, excessive crushing of constituents and specimen cracking are observed for foams with untreated and treated cenospheres respectively as seen in Figure 3.7b-e. In addition, the stress-strain curves of unconditioned EXX-T type syntactic foams show lower fracture strain values as compared to unconditioned EXX-U. Relatively higher brittleness owing to silane coating on cenospheres increases overall brittleness of composite foams reducing the fracture strain for EXX-T. Nevertheless, in the case of coated cenospheres, mean particle diameter appears to influence the higher stiffness of the composites resulting in earlier crack initiation in the direction of compression. This might lead to the formation of relatively larger fragments in EXX-T. Such situations are preferred while designing core for sandwich structures. In the case of arctic exposed samples, fracture strain values are similar between EXX-T and EXX-U type syntactic foams.

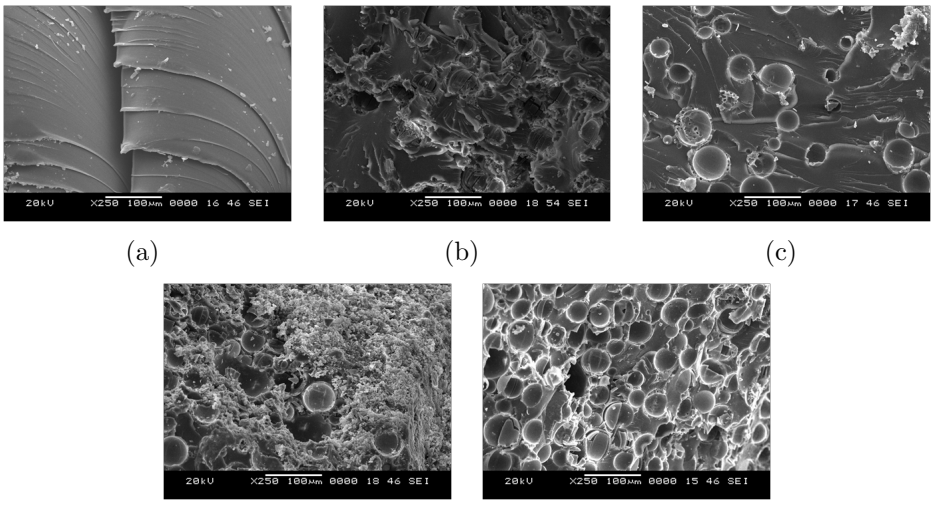

Figure 3.7: Micrographs of (a) Neat epoxy resin (b) E20-U (c) E20-T (d) E60-U and (e) E60-T post compression room temperature tests.

Fracture surfaces of representative syntactic foams are shown in Figures 3.8 and 3.9, where an extensive cenosphere damage is observed during compressive fracture of the EXX-U material. Such fracture of microballoons and generation of debris has also been observed in epoxy matrix syntactic foams [45]. EXX-T foams have lesser debris at both lower and higher volume fractions. Good interfacial bonding between the constituents due to silane treatment imparts higher resistance to the particles against debris formation under compressive loading. At E60-T, majority of the cenospheres are partially fractured retaining their original locations resulting in higher strength values compared to E60-U foam. Though the compressive strength shows a decreasing trend with increasing filler content, specific values are comparable or marginally better than that of the neat resin counterparts. Such situations are highly desirable in structural components used in marine applications.

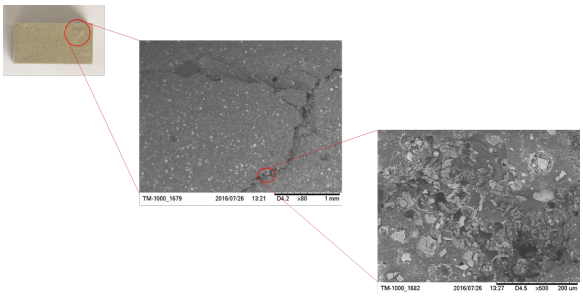

Figure 3.8: E40-U compression specimen schematic post arctic condition test.

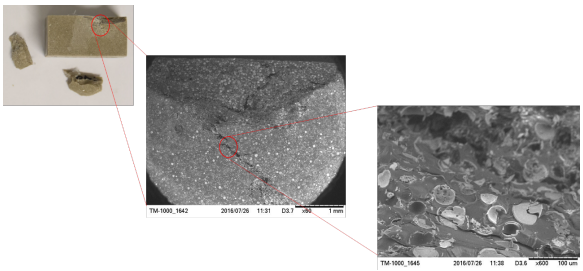

Figure 3.9: E40-T compression specimen schematic post arctic condition tests.

3.4 Conclusion

Compressive properties of untreated and treated cenosphere/epoxy foams under room and arctic temperatures are analyzed in the present work. It is observed that the cenosphere/epoxy foams with untreated and treated fillers manifest lower strains to failure under compressive loading at room temperature conditions as compared to neat epoxy samples. All foam compositions show an increase in compressive modulus compared to that of the neat resin. The results show that epoxy matrix syntactic foams with treated cenospheres have promise for structural application at room temperatures. Significantly higher specific compressive moduli and marginally higher specific strength make treated cenospheres/epoxy syntactic foams (EXX-T) a viable material for marine applications.

Further, these foams were subjected to compressive loading at -60^{o}C to explore the feasibility of using them in arctic environment. Similar to room temperature tested samples, all cenosphere/epoxy foams with treated and untreated fillers exposed to arctic conditions

demonstrated lower failure strains as compared to neat epoxy, but also compared to its unconditioned counterpart. It was observed that for the compression specimens, the modulus of elasticity decreased for arctic specimens compared to the unconditioned (dry) specimens. However, an overall increase in compressive strength was observed when tested under in-situ arctic condition. After examining the behavior of all samples, it was observed that the conditioning of specimens under extreme low temperatures caused the material to reduce their compressive modulus. Also, the syntactic foams behaved in a brittle manner causing drastic failure under in-situ compression testing. This can represent a challenge when using this type of foams since no signs of deterioration/damage can be observed before failure occurs.

Chapter 4

Flexural Behavior of Surface Modified Cenosphere/Epoxy Syntactic Foams in Arctic Environment

4.1 Introduction

Sandwich structures with foam cores are of current interest to in applications like naval crafts. These foam cores are typically made from closed-cell and low-density polymers and a sandwiched between fiber-reinforced polymeric composite facings. Such sandwich constructions are extremely lightweight, which increase the buoyancy of ship-structures. However, extended period of sea environment exposure results in mechanical property degradation due to moisture absorption and temperature variations in such materials in marine applications. Structural components in marine applications face these major concerns and are the focus of the research presented in this paper. Syntactic foams are a special class of composite foams, which consist of hollow microspheres dispersed in a matrix resin [23]. The spectrum of engineering applications of these foams is very broad as elaborately discussed in Gupta et al. [68]. Hulls, ribs and decks of boats are the initial applications of syntactic foams in marine structures. Nevertheless, syntactic foams are also utilized in remotely or humanly operated structures of deep sea vehicles. Syntactic foams are promising material systems for thermal insulation in deep sea oil pipelines.

Developing structure-property correlations and understanding failure mechanisms for tailoring syntactic foam properties for various applications has been extensively dealt with in the past decade[32, 69, 36, 70]. Thermal and electrical properties of syntactic foams [33, 34, 35, 25] have also been investigated in addition to mechanical properties. Further, reinforced syntactic foams with micro and nanosized fibers and particles have been extensively studied, which were beneficial towards tailoring the properties as compared to plain syntactic foams [71, 72]. Recently, thermoplastic foams were developed using

industrial scale injection molding machine and characterized for mechanical properties [31, 58, 59, 73, 74, 54, 55].

Syntactic foams are tested under three-point bending in either flexural [37, 38, 39, 40] or short beam shear test configurations [41, 42, 43] in the recent past. The relationship of volume fraction and surface modification of fillers with the flexural modulus is often complex. Possibility of stiffening the matrix with low density hollow particles depends on the relative modulus of the particle material, geometrical parameters and the matrix properties. Effects of particle wall thickness and interfacial bonding between the constituents also have significant effects on flexural properties. Published literature reports several experimental and analytical studies on hygrothermal [50, 46, 52], impact [53], microstructural characterization [75, 44] and effect of polymer cure cycle [76] of syntactic foams. In many of these studies, the effect of filler content variation on the mechanical properties is elaborately discussed. Wall thickness variations and built-in porosities in walls of hollow particles in cenosphere/epoxy foams makes structure-property correlations quite complex and challenging to address especially with additional temperature effects like in arctic conditions. Since syntactic foams are being commonly used under extreme environmental conditions like in marine vessels, it is necessary to understand their mechanical properties in arctic conditions. Also, environmental temperature significantly affects the water absorption and mechanical properties of syntactic foams [47, 77]. However, the concerns of low temperature effects on mechanical properties need to be addressed.

Engineered glass microballoons as filler materials have been widely studied [25, 26]. Sodalime-borosilicate glass is a major constituent of these engineered glass particles. Degradation of such syntactic foams has been reported recently due to dealkalization of glass [27]. Fly ash, an industrial waste material and a potential environmental pollutant, also contains hollow particles called cenospheres mainly made of alumina and silica. Coal combustion in thermal power plants generates cenospheres as by-product. Though, they have numerous defects on and in their walls with marginal deviations from perfect sphericity, the aluminosilicate composition might compensate the limitations caused by such defects. Further, fly

ash cenosphere properties have been found to be in the range of commonly used glass microballoons. Developing utilitarian syntactic foams with this industrial waste can help the environment, minimize landfill burden and create foams with better properties [28, 29, 30]. The current work uses fly ash cenospheres for manufacturing syntactic foams.

Majority of studies on the mechanical properties is carried at room temperature (RT) [78, 79]. However, for marine vessel that operate in the arctic or antarctic oceans, it is critical to investigate these materials in such harsh environment of sub-zero temperatures. The effects of arctic environment on cenosphere/epoxy foams has not been studied before, and is crucial for marine structural components operating in Arctic regions. The present study explores this possibility by investigating the flexure behavior of syntactic foams owing to changes in operating temperatures. Hollow fly ash cenospheres, epoxy matrix, surface modification of filler and volume fractions are held constant while altering the exposed temperature. Thereby, changes in the fracture pattern are attributed to the operating temperature. The behavior of syntactic foams in such temperatures can be explored by such an investigation, which has not been reported in the literature yet. The novel aspects of the present study include (a) use of industrial waste fly ash cenospheres for developing eco-friendly syntactic foams and (b) structure-property correlations at arctic conditions along with the influence of filler (cenosphere) surface modification.

4.2 Materials and Methods

4.2.1 Constituents

Fly ash cenospheres of CIL 150 grade used as filler particles are procured from Cenosphere India Ltd., Kolkata, West Bengal, India. These are hollow particles primarily obtained as by-product from coal plants. Table 4.1 presents the chemical, physical and sieve analysis details of cenospheres in as received condition. Cenospheres primarily comprise of alumina, silica, calcium oxide and iron oxides as observed from this table. Lapox L-12 epoxy resin with K-6 hardener, supplied by Atul, Valsad, Gujarat, India constitutes the matrix resin. Syntactic foams are fabricated with two configurations: 1) with as received cenospheres

and 2) surface modified cenospheres. Cenospheres are coated with Silane using 3-Amino propyl tri ethoxysilane (APTS), which is procured from Sigma Aldrich, Bangalore, India. At least five specimens are tested in flexure under room and arctic temperatures each.

Table 4.1: Chemical, physical and sieve analysis details of cenospheres

Physical properties	Chemical analysis	Sieve analysis			
True particle density	920 kg/m^3	SiO_2	52-62%	+ 30 # (500 μm)	Nil
Bulk density	400-450 kg/m^3	Al_20_3	32-36%	+ 60 # (250 μm)	Nil
Hardness (MOH)	5-6	CaO	0.1-0.5%	+100 # (150 μm)	Nil
Compressive strength	180-280 kg/m^3	Fe_20_3	1-3%	+150 # (106 μm)	0-6%
Shape	Spherical	TiO_2	0.8-1.3%	+ 240 # (63 μm)	70-95%
Packing factor	60-65%	MgO	1-2.5%	- 240 #	0-30%
Wall thickness	5-10% of shell dia.	Na_2O	0.2-0.6%		
Color	Light grey - light buff	K_2O	1.2-3.2%		
Melting point	1200 - 1300 °C	CO_2	70%		
pH in water	6-7	N_2	30%		
Moisture	0.5% max.				
Loss on ignition	2% max.				
Sinkers	5% max.				
Oil absorption	16 - 18 g/100 g				

[1]As specified by supplier

4.2.2 Surface modification of cenospheres

Due to the hollow nature of cenospheres, volume fraction and size play a critical role in lightweighting. In addition, the interaction between cenosphere and epoxy plays a major role in the load transfer mechanism between the constituents [57]. The mechanical properties of cenosphere reinforced polymeric composites are inferior owing to poor interfacial interactions between the hydrophilic cenosphere surface and hydrophobic polymer. Silane coupling agents are typically used as adhesion promoters between these constituents. In the current work, cenospheres are surface treated with silane. Cenospheres weighing 50 g are mixed into 100 ml solution of water/ethanol (20:80 wt. %). Further, 2% by volume of APTS is added to this solution and continuously stirred for 30 minutes at 80°C in a microwave reactor (Enerzi microwave systems, Bangalore, India). The resultant mixture is filtered, washed at least three times in a water/ethanol solution and then dried in an oven

to extract the coated cenospheres.

4.2.3 FTIR, XRD and particle size analysis

Cenospheres are analyzed using FTIR spectroscopy (JASCO 4200, Japan, Automated Total Reflection mode, wave number 4000 to 650 cm^{-1}) to confirm the silane coating. X-ray diffractograms are obtained for 2Θ values using DX GE-2P, JEOL, Japan having Nickel filter material with scanning speed of 2°/min and Cu Kα (λ=1.514 A°) radiation. Particle size and shape analysis is conducted using a Sympatec (Pennington, NJ) QICPIC high speed image analysis system [59, 58].

4.2.4 Sample preparation

Syntactic foams are fabricated by mechanically mixing cenospheres in a desired volume fraction with Lapox L-12 epoxy resin and K-6 hardener at room temperature. The mixture is then gently stirred to obtain a homogeneous and uniform slurry. Hardener is added by 10 wt.% and finally the mixture is degassed for 10 min prior to casting in aluminum molds. The cast slabs are cured at room temperature for 24 hours and post cured at 90℃ for 3 hours. Three different cenosphere foams are fabricated by maintaining the cenospheres content at 20, 40 and 60 vol.% in epoxy matrix. This procedure is adopted for both as received and silane treated cenospheres. Additionally, neat resin specimen, i.e., without any filler in the matrix, is also fabricated which serves are the baseline material system for comparative studies. Samples are named according to the convention EXX-Y, where E denotes epoxy resin, XX is the volume fraction of cenospheres and Y represents filler modification condition (U denotes untreated and T represents silane treated cenospheres). Cast slabs are trimmed using diamond saw cutter to confirm to the dimensions as mentioned in ASTM D790 (flexural). The densities of all the samples are experimentally measured using the procedure outlined in ASTM D792-08 and the average values are reported.

Theoretical density is computed using the rule of mixture given by,

$$\rho_c = \rho_f V_f + \rho_m V_m \tag{4.1}$$

where, ρ and V are density and volume fraction, respectively. Subscripts c, f and m denote composite, filler and matrix, respectively. Furthermore, the void content (Φ_v) is estimated using theoretical (ρ^{th}) and experimental (ρ^{exp}) densities and is given by [36, 38],

$$\Phi_v = \frac{\rho^{th} - \rho^{exp}}{\rho^{th}} \tag{4.2}$$

4.2.5 Arctic Conditioning

To the knowledge of the authors, there is no standard for arctic exposure studies. Therefore, the procedure for conditioning of specimens was developed in-house and similar to that of initial conditioning for water uptake measurement standards (ASTM C272 and D5229). Prior to any type of conditioning and testing, the syntactic foams are oven dried for 24 hours to eliminate any moisture absorbed during processing and handling. Further, five samples each corresponding to different volume fractions for both untreated and treated categories are placed in a Thermo Scientific TSU Series -86°C Upright Ultra-Low Temperature Freezer, which is maintained at -60°C. All specimens are conditioned for 57 days, after which the specimens are tested under in-situ arctic conditions (-60°C). The procedure for obtaining the mechanical properties of the syntactic foam samples is discussed in the following section.

4.2.6 Flexural Test

All the specimens are tested at room (30°C) and arctic temperatures (-60°C) using Instron 5969 Tabletop Universal Testing system and following the ASTM D790 standard for three point bend (flexural) tests. A crosshead displacement of 1.4 mm/min is maintained for evaluating the flexural strength and modulus of elasticity in flexure. Span-to-depth ratio of 16:1 is maintained for all the samples considered in this study.

4.3 Results and Discussions

4.3.1 Material Processing

In the current study, fly ash cenospheres are used in as received (untreated) and silane modified (treated) conditions. FTIR results for untreated and silane treated cenospheres are presented in Figure 4.1(a). The spectrum confirms the presence of a silane surface layer. The characteristic peak of 3-aminopropyl triethoxy silane has a band lying in around 2900 cm^{-1} representing a vibration absorbing peak of C-H bond, which belongs to CH_3. In the FTIR spectra, the peak absorbed for fly ash cenospheres with surface-modification occurs at 2929 cm^{-1}. This peak is absent in the spectrum for untreated fly ash cenospheres, which suggest that the observed peak corresponds to the characteristic peak of 3-amino-propyl triethoxy silane [80].

Figure 4.1(b) depicts the XRD diffraction results of as received and silane modified cenospheres. Untreated and treated fly ash cenospheres have a dominant peak at 26.6 and 26.04, respectively, with numerous other small peaks as it consists of mainly metal oxides, predominantly SiO_2 and Al_2O_3. The X-ray diffraction pattern of mullite is very similar to that of sillimanite. Sillimanite is a commonly occurring alumina silicate mineral stable at high pressures, a 1:1 ratio of silica to alumina. Mullite is the only stable intermediate phase in the alumina-silica system at atmospheric pressure [81]. The chemical formula of mullite is $3Al_2O_3{+}2SiO_2$. The main compounds of fly ash cenospheres are SiO_2 and Al_2O_3. The total sum of percentages of SiO_2, Al_2O_3 and Fe_2O_3 is nearly 90% of the total composition. Other compounds such as K_2O, MgO, CaO, TiO_2 and Na_2O are present in trace quantities.

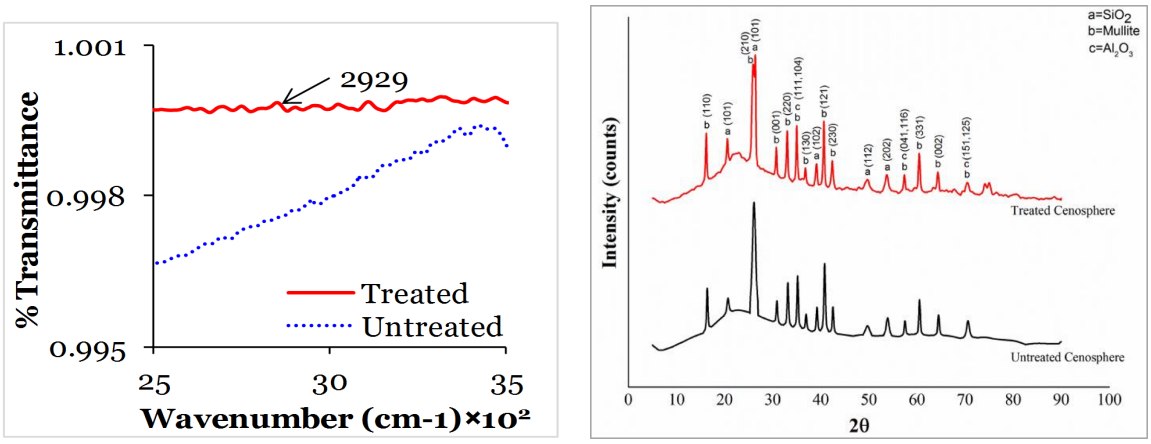

(a) (b)

Figure 4.1: (a) A section of the FTIR spectra of untreated and silane treated cenospheres [44]; (b) X-ray difftractogram of cenospheres

Figure 4.2(a-b) present the micrographs of untreated and treated cenospheres, respectively. The coating layer is not visibly identifiable in the micrographs due to its small thickness, despite FTIR results confirm silane presence on cenospheres. Surface morphology is not uniform for fly ash cenospheres due to variations in sphericity and the presence of numerous defects as seen in these micrographs. A high magnification micrograph of one broken cenosphere is shown in Figure 4.2(c). Porosity and irregular wall thickness is clearly evident in Figure 4.2(c). Porosity in the cenosphere walls might lead to lower mechanical properties as compared to non-porous fillers. Such variations can lead to deviation of the experimental observations from that predicted by empirical and/or mathematical models.

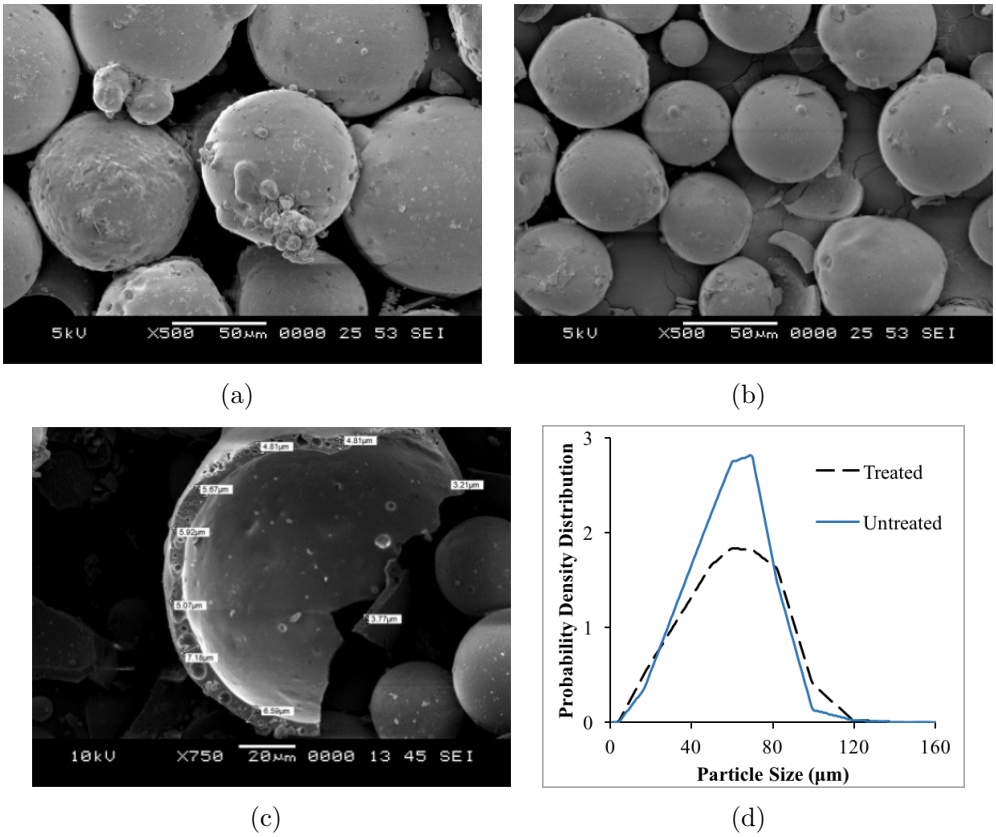

Figure 4.2: Cenosphere micrographs of (a) untreated (b) treated and (c) one such broken treated particle. Wall thickness variations and built-in porosity in fly ash cenospheres are clearly evident from these micrographs; (d) Particle size analysis of untreated and treated cenospheres

Untreated and treated cenospheres are subjected to particle size analysis and the results are shown in Figure 4.2(d). Untreated and treated cenospheres registered X50 median particle sizes of 48.82 and 55.22 μm, respectively, confirming an increase in the average diameter owing to silane treatment. Broader peak is seen in the case of treated particles. Densities of as received and treated cenospheres are measured to be 0.920 and 1 kg/m^3. Sphericity of cenospheres is observed to be in the range of 0.6-0.9, which is reported in a previous study [58]. Shift in the curve for treated particles can also be attributed to particle coating. Also, in Figure 4.2(d), a considerable extension at the tail end of the curve is observed for treated and untreated particles indicating a small amount of cluster

formation. Shear forces induced during manual stirring is expected to disperse some of these clusters formed.

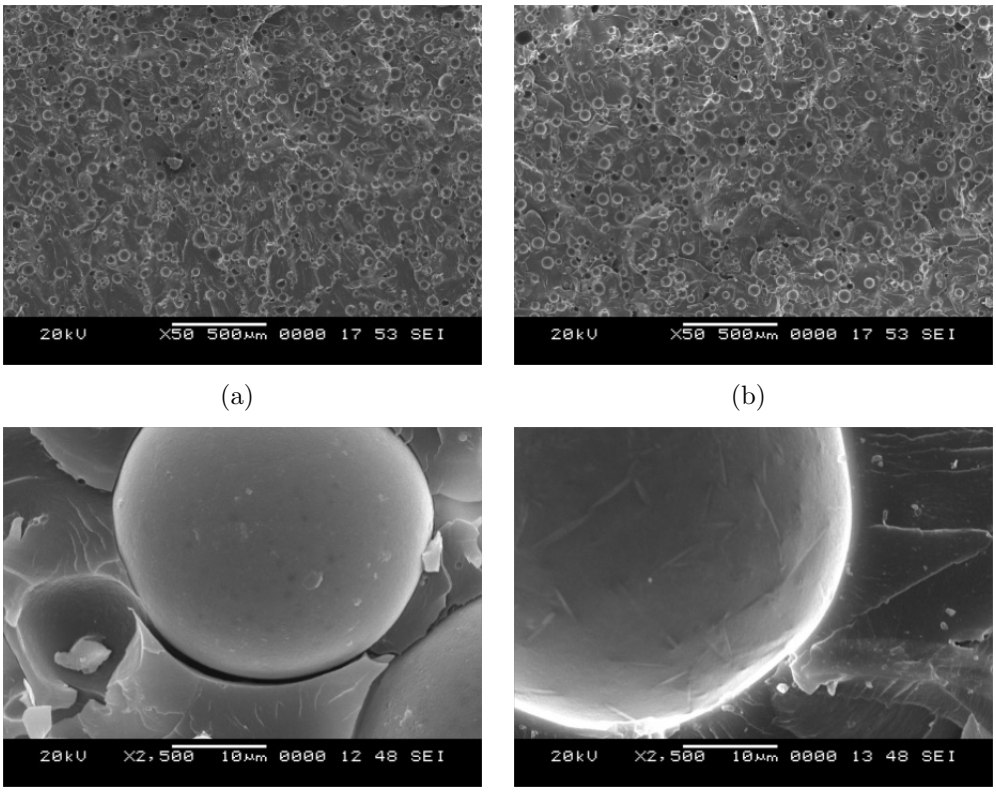

Figure 4.3: Micrograph of as cast (a) E20-U (b) E20-T foams showing uniform dispersion of cenospheres. Lack of bonding for E20-U is seen in (c) while good interfacial bonding is evident from (d) due to silane treatment in E20-T

Synthesizing syntactic foam composites with uniform dispersion of cenospheres, lower cluster formation and minimum particle failure in the matrix during processing is a challenging task. Further, particles survival from fragmenting is a crucial parameter as broken particles adversely affect the mechanical properties. These fragments increase stress concentration and the density of the composites fabricated. Nevertheless, all of the above mentioned factors are dealt effectively with the manual stirring approach during fabrication, which minimizes particle failure to a great extent and facilitates uniform dispersion.

Thereby, in the current work manual stirring is used to fabricating cenosphere/epoxy foams. Micrographs of as cast cenospheres/epoxy foams are shown in Figure 4.3. Uniform dispersion of hollow cenospheres, both untreated and treated, in the matrix is observed in Figure 4.3(a-b), demonstrating the feasibility of using manual stirring for fabricating these syntactic foam composites. Further, particle clusters are not observed in the foams with treated cenospheres (Figure 4.3b) as anticipated from Figure 4.2(d).

Clusters are expected to be broken effectively due to the shear forces induced during the stirring of the cenospheres/epoxy slurry. Interfacial adhesion (bonding) between the epoxy resin and the as received cenospheres is observed to be poor as seen in Figure 4.3c. Silane modification of cenospheres shows good adhesion between the constituents (Figure 4.3d). Improvement in the interfacial bonding is expected to improve the load transfer from the matrix to the particles, which subsequently will assist in improving the overall mechanical properties of the syntactic foams. Failure mechanisms in foam composites are governed by the interface topology. Flexural and tensile properties are strongly affected by the interfacial bonding strength [59, 58, 60, 61] as interfacial cracks in the form of debonding can occur under such loading conditions. On the other hand, compressive properties are less sensitive to the extent of bonding between the matrix and cenospheres [62, 63]. Non-uniform coating layer on cenospheres renders the comparison of mechanical properties challenging [38] and is not the scope of the current work.

Quality and the mechanical properties of syntactic foams depend on the survival of the hollow cenospheres and the void content due to entrapped air during processing. Therefore, it is necessary to quantify and correlate these parameters with the properties being investigated. Table 4.2 presents the density and void content estimations. Theoretical density values are higher compared to experimental ones as observed from Table 4.2. Lower experimental densities of composites as compared to the theoretical ones is attributed to the air entrapped in matrix during the process of mechanical mixing of cenospheres in the matrix resin. The presence of very few entrapped air pockets are seen in Figure 4.3a-b for typical syntactic foam. Such entrapped air pockets are undesired due to their adverse

affects on the mechanical properties and are referred to as voids.

Table 4.2: Density and Void volume fraction of syntactic foams.

Material	ρ^{th} (kg/m^3)	ρ^{exp} (kg/m^3)	ϕ_v (%)	Weight saving (%)
E	—	1.1920 ± 0.410^{-3}	0.34	—
E20-U	1.1376	1.1296 ± 0.910^{-3}	0.70	9.06
E40-U	1.0832	1.0647 ± 1.210^{-3}	1.71	11.45
E60-U	1.0288	1.0283 ± 1.810^{-3}	0.05	16.12
E20-T	1.1536	1.1331 ± 1.210^{-3}	1.78	5.09
E40-T	1.1152	1.0739 ± 2.110^{-3}	3.70	8.78
E60-T	1.0768	1.0556 ± 3.510^{-3}	1.98	11.91

Table 4.2 shows the variation of void content with varying filler content percentages. It is observed that the void content generally increases with increasing filler content except at the highest filler content of 60 %. The presence of such voids reduces the matrix content, assuming that all the voids replace the matrix. The amount of matrix present at 60 vol. % filler content is much lesser as compared to other compositions resulting in much lower void content at highest filler loading. Densities of foams with treated cenospheres registered higher values for all the compositions as compared to untreated counterparts. As observed before, silane coating on as received cenospheres increases the effective mean diameter (Figure 4.2d) consequently increases their density. Standard deviations of the densities are observed to be in a very narrow range (Table 4.2) affirming consistency in specimen processing. Further, the potential of weight saving as compared to neat epoxy samples are shown in Table 4.2. Lower effective densities of syntactic foams with untreated cenospheres noted to have better weight saving potential. Specific mechanical properties are worth considering for exploiting these lightweight cenosphere/epoxy foams in naval applications. It would be an interesting task to understand and analyze the effect of arctic environment on such abundantly available untreated/treated hollow fly ash cenospheres to propose suitable applications.

4.3.2 Flexural Modulus and Strength

Representative stress-strain responses are shown in Figure 4.4. Irrespective of the testing environment, all types of syntactic foams fail in brittle mode in the post peak region. Foams with untreated cenospheres exhibit non-linear behaviour at room temperature as seen from Figure 4.4a as compared to Figure 4.4b. Poor adhesion between the constituents (Figure 4.2c) resulting in an unconstrained matrix flow around the cenosphere particles and relatively easier displacement of cenospheres within the matrix under applied load might be the reason for such behavior. Due to better adhesion between the treated cenospheres and matrix, the response of the syntactic foams are dictated by the cenospheres, resulting in a linear stress-strain response in the pre peak response as observed in Figure 4.4b. In the case of the arctic conditioned specimens, the stress-strain response curves presented two linear regions. The second linear region is used for all calculations to determine the stiffness and strength properties. Failure response is found to be similar in both the arctic conditioned and unconditioned samples, which resembles brittle fracture as mentioned earlier.

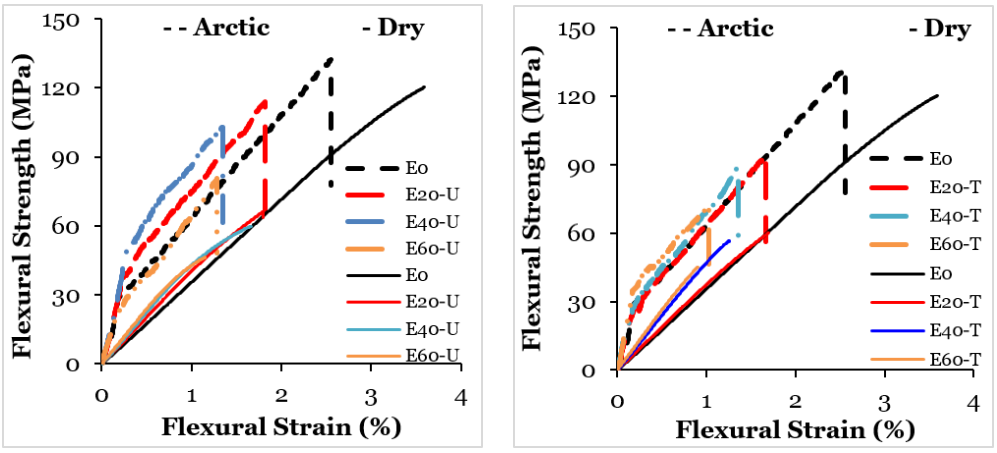

(a) (b)

Figure 4.4: Representative stress-strain curves obtained in the flexural testing of syntactic foams containing 20, 40 and 60 volume % (a) untreated and (b) treated cenospheres

Table 4.3: Flexural Modulus and Strength properties of syntactic foams.

Material	Flexural (MPa)			
	30°C		-60°C	
	Modulus	Strength	Modulus	Strength
E	3436.98 ±68.74	120.29 ±2.41	4226.29 ±301.50	126.17 ±15.40
E20-U	3729.55 ±74.59	60.09 ±1.20	4264.81 ±281.71	93.82 ±14.91
E40-U	4431.51 ±88.63	56.74 ±1.13	5414.75 ±446.30	100.34 ±3.32
E60-U	4755.30 ±95.11	45.23 ±0.90	4841.14 ±864.01	75.78 ±14.10
E20-T	3958.71 ±79.17	66.23 ±1.32	4661.66 ±323.56	89.49 ±6.79
E40-T	4746.83 ±94.94	59.82 ±1.20	4058.76 ±732.23	77.60 ±8.74
E60-T	5196.11 ±103.92	48.28 ±0.97	4771.89 ±463.43	72.50 ±4.36

Flexural modulus and strength values are computed for each case using the experimentally obtained load-displacement data. Figure 4.5a-b display the effect of volume fraction and surface modification of cenospheres on the flexural modulus of syntactic foams. Modulus increases with increasing filler content for the foams with untreated and treated cenospheres (Table 4.3). EXX-T foams registered higher moduli at all the volume fractions (particle content) as compared to EXX-U ones at room temperature. Further, all compositions of syntactic foams exhibit higher elastic modulus than the neat resin. These observations are similar to the results obtained in tensile and flexural testing of syntactic foams [82, 83, 84].

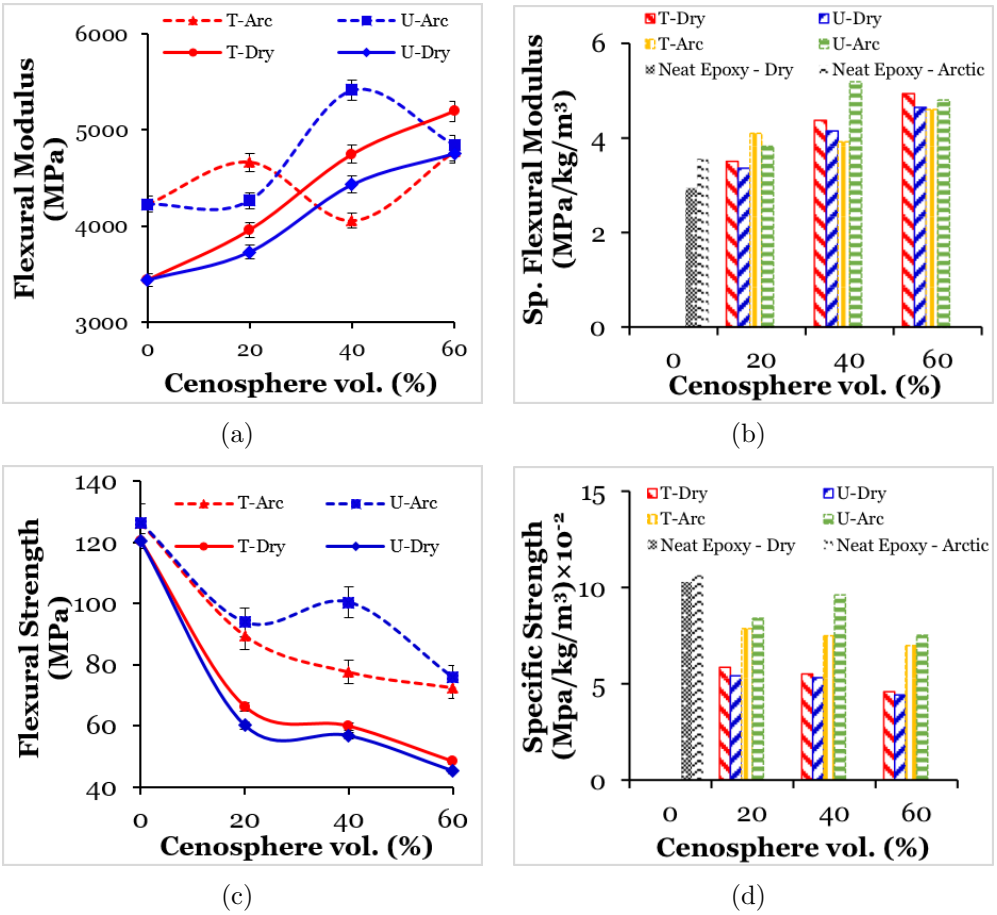

Figure 4.5: Experimentally measured flexural (a) modulus (b) specific modulus (c) strength and (d) specific strength of syntactic foams

As presented in Figure 4.5b, all the compositions of syntactic foams exhibit a higher specific elastic modulus as compared to neat resin samples. Hence, 12-16% weight saving in structures can be obtained by using cenosphere/epoxy syntactic foams with superior specific properties making these foams suitable for naval applications. Such weight saving is especially desirable in marine applications where buoyancy is one of main criteria in designing structures.

Flexural strength of cenosphere filled epoxy composites is exhibited by Figure 4.5c-d. Flexural strength for both EXX-U and EXX-T foams is less than the strength of the neat resin at room temperature and arctic conditions. Specific strength shown in Figure 4.5d and

in the fracture strain as seen from Figure 4.4 exhibit similar trend. However, foams with treated fillers have registered better response under room temperature test whereas opposite trend is noted for arctic conditioned samples. Foams with untreated filler registered better response in arctic environment. As these foams can be used as core in sandwiches, they do not limit the applicability in marine structures due to lower fracture strength and strains. The flexural strength appears to have a significantly stronger dependence on the filler content while marginal influence on the particle surface modification. Higher brittleness at the cenosphere-epoxy interface and silane modified particles might have played a significant role for such insensitivity. Increasing filler content decreases strength implying reduction in foam strength owing to lower matrix content. These findings, along with the fracture features presented in Figure 4.6, suggest that interface debonding followed by matrix cracking is the primary mechanism of syntactic foam failure in EXX-U foams. Whereas, particles cracking (Figure 4.6e) is the failure source for the foams with treated cenospheres.

When comparing arctic conditioned samples to unconditioned (dry) samples, an increase in its flexural modulus of elasticity can be observed between 2-23% for untreated specimens. In the other hand, in the case of treated samples it was observed that the modulus increased only for 20 vol. % samples by 18% while causing a reduction in its modulus between 8-15% as the filler content increased. For the case of flexural strength, an increase between 5-77% was observed for untreated cenospheres and 5-50% for treated cenospheres in in-situ arctic samples. The arctic conditioning to which samples were subjected caused the samples to become more rigid causing an increase in their flexural modulus and strength values.

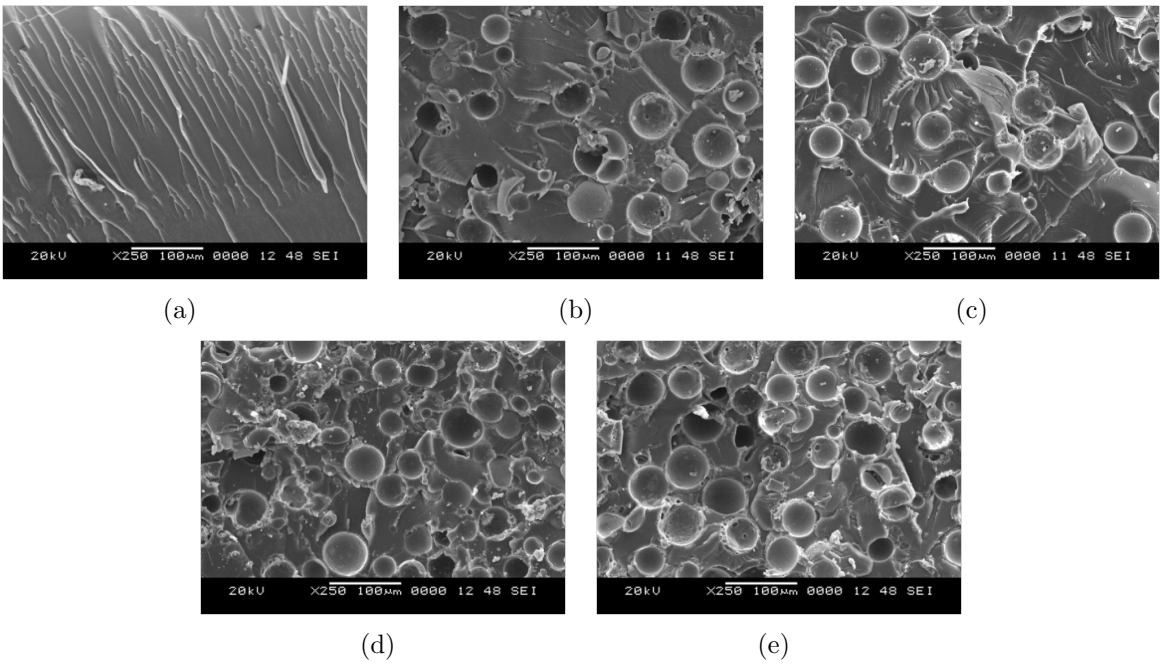

(a) (b) (c)

(d) (e)

Figure 4.6: Micrographs of (a) Neat epoxy resin (b) E20-U (c) E20-T (d) E60-U and (e) E60-T post flexure room temperature tests

For the case of arctic conditioned samples, the degradation caused by the environmental exposure can be observed to be more predominant in the 40 vol. % samples. A combine effect between the matrix and the cenospheres exists in the mechanical properties of the samples. Given that the interphase between matrix and cenospheres has a higher influence in the material properties for this configuration, a higher degradation of this region may lead to a decrease in its properties. Treated cenospheres samples have better adhesion between matrix and cenospheres but the exposure to temperatures of -60°C results in higher degradation of the interphase as comparison to untreated samples leading to a higher difference observed in Figure 4.5a and Figure 4.5c. On the other hand, 20 vol. % is matrix dominated and 60 vol. % is dominated by the cenospheres, and the influence of the interphase is not significant at these two volume percentages.

The fracture features of neat epoxy and syntactic foams containing 20 and 60 vol. % of untreated and treated cenospheres at room temperature tests are presented in Figure

4.6. The micrographs were taken post flexure test on the fractured surfaces. Absence of debris is observed in all these micrographs indicating tensile fracture [38]. Such a feature is also noted in syntactic foams with cenospheres in thermoplastic (HDPE) matrix [59, 58] like in thermosetting (epoxy) ones. In flexural loading conditions, absence of debris on the fracture surface is due to crack growth from the tensile side of the sample which governs the brittle mode of fracture. Extensive plastic deformation marks are seen on neat epoxy samples without any debris as observed in Figure 4.6a. Interaction of these deformation waves with untreated and treated cenospheres are worthy of investigation. Figure 4.6b and Figure 4.6d show debonding and displacements of cenospheres from the resin matrix during the deformation and fracture as compared to EXX-T (Figure 4.6c and Figure 4.6e). This implies that most of the stress in the composite is withstood by the matrix material in foams with treated filler that determines the composite failure strength. This is obvious owing to good interfacial bonding between the constituents in EXX-T (Figure 4.3d). Strength values of foams with treated particles are higher compared to untreated ones for all the compositions tested at room temperature. Constrained matrix movement around relatively tougher treated particles registered higher strength values. With increasing filler content variations in particle sphericity, wall thickness and built-in porosities (Figure 4.2c) induce additional stress concentration suppressing silane coating effect and hence lowers their strength. Though these foams have limitations in strength, they are promising in terms of high stiffness if used in sandwich composites as core materials.

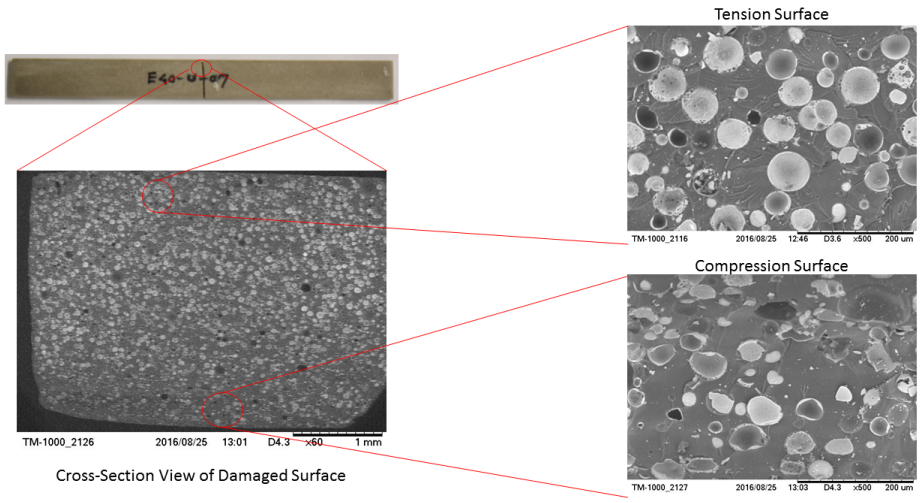

Figure 4.7: E40-U Flexural Specimen Schematic post arctic condition test

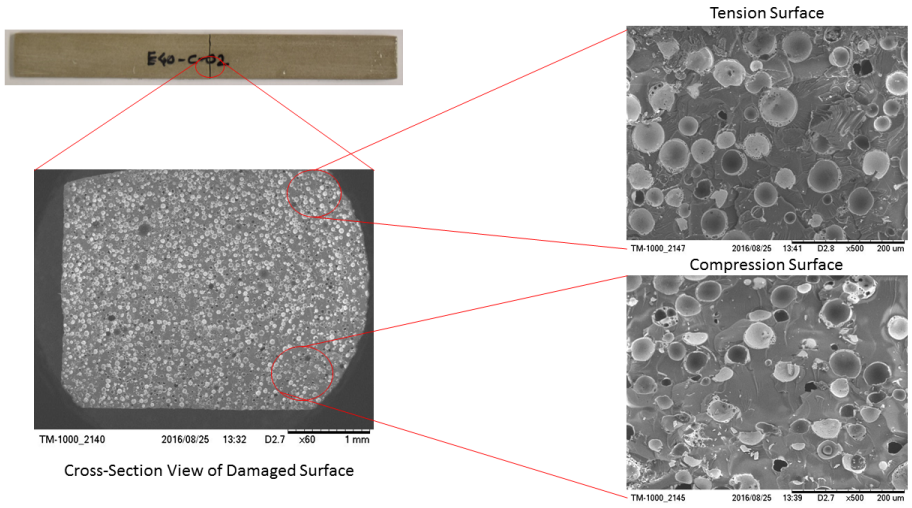

Figure 4.8: E40-T Flexural Specimen Schematic post arctic condition test

Fracture features for syntactic foams containing 40 vol. % for untreated and treated cenospheres in arctic environment can be observed in Figure 4.7 and Figure 4.8. All micrographs are obtained at the fracture surfaces post flexural tests. Similar fracture features are observed for both treated and untreated samples. Like for unexposed samples, tensile fracture is also observed in arctic conditioned samples.

4.4 Conclusions

Flexural behavior of untreated and treated cenosphere/epoxy foams under room and arctic temperatures are analyzed in the present work. Experimental results on a variety of compositions show that the specific flexural modulus of these lightweight composites is considerably higher than the neat resin. Flexural modulus of these foams can be effectively tailored by filler surface modification and varying filler volume fraction. On the other hand, the flexural strength is primarily influenced by the resin content in foams. It is observed that the flexural strength decreases as the filler content increases. Lack of interfacial bonding between the foam constituents limits the load transfer at the interface for composites with untreated cenospheres. Similar trend is observed for treated particle foams owing to geometrical imperfection with such naturally available fillers. Further, these foams are subjected at -60°C to explore the feasibility of using them in arctic environment. Similar to room temperature tested samples, all cenosphere/epoxy foams with treated and untreated fillers exposed to arctic conditions demonstrated lower failure strains as compared to neat epoxy. Arctic exposed samples reported a slight increase in their modulus of elasticity as compared to room temperature samples.

Key finding were as follows:

1. An increase in flexural modulus was observed in syntactic foams at room and arctic temperature as compared to neat resin, whereas the flexural strength decreased. Reduction in flexural strength can be attributed to the introduction of weak regions in the matrix material due to the addition of cenospheres.

2. An increase in flexural modulus between 2-23% was recorded for syntactic foams with untreated cenospheres under arctic conditions as compared to the ones tested at room temperature.

3. Flexural strengths increased in the range of 5-77% for arctic exposed syntactic samples as compared to room temperature ones. This is accredited to the increase in rigidity

experienced by the samples when exposed to arctic temperatures.

4. Surface treatment of cenospheres did not provide significant improvement to the flexural modulus or strength under arctic temperatures.

5. Finally, arctic conditioning and in-situ exposure rendered the syntactic foams brittle, causing sudden failure in the post peak regime.

After examining the behavior of syntactic foams in arctic environment, it is concluded that the flexural modulus increases with arctic exposure and filler volume percentage. These materials systems have great potential to be used as core materials for sandwich construction in such extreme conditions, where a significant improvement in the flexural modulus can be achieved. However, due to inferior flexural strengths, using syntactic foams only in primary load bearing structures without other high strength materials, like carbon or glass facings, is not suggested.

Chapter 5

Computational Modeling of Syntactic Foams During Compression

5.1 Introduction

In the recent years, the interest to use composites materials to replace conventional engineering materials for naval applications has been increasing. Sandwich composites materials conformed of a polymeric matrix core reinforced with small particulates are of interest thanks to its tailor made properties for naval applications. These cores are made from closed-cell and low-density polymer composites placed between fiber-reinforced polymeric composite facings. These components are characterized by being extremely lightweight which can help increase the buoyancy of the craft when employed in the ship-structure design. Syntactic foams are a special class of sandwich cores considered for marine applications. They are formed by combining a polymeric matrix and microballoons, which are hollow spheres mostly made out of silica and alumina filled with air or an inert gas. Earlier researchers such as Marur [85] and Antunes et al. [86] have used numerical approximations and numerical models respectively to predict the behavior of the syntactic foam materials and therefore optimize its mechanical properties. But, seldom work has been reported that discusses the computational modeling of these. With the overarching goal of improving the performance of sandwich composites and the necessity to reduce the time and cost associated with testing and validation of materials, the implementation of computational modeling can help the researcher by providing a better understanding of the material behavior. The objective of this paper is to develop a computational model capable of predicting the mechanical behavior of syntactic foams.

5.2 Model Overview

5.2.1 Case Studies

Computational 3D models were developed for two different volume fractions. In this case, only 20 vol.% and 40 vol.% models were considered. Besides, for each volume fraction, four distinct size models were examined. The representative volume elements (RVE) consisted of 0.25 mm, 0.5 mm, 0.75 mm, and 1.0 mm. Also, for the case of 40 vol. % a packing study was performed in order to examine the effect that different packing of sphere might have in the model.

Computational models were subjected to 1% total deflection in compression in order to capture the linear-elastic behavior of the model. In all cases, perfect bonding between the spheres and the matrix was considered. Mechanical properties for each case, 20 vol. % and 40 vol. %, were validated using experimental data previously obtained.

In addition to the 3D models, a 2D damage prediction model was developed using the same characteristics as for the previous models (20 vol. % only). The purpose of the model is to examine how the model will behave during the plastic regime showing the initial stages of failure/fracture and how its response compare to experimental results. The total displacement the model was subjected was of 2% total deflection in compression.

5.2.2 Random Distribution of Spheres

A MATLAB script was used to generate the dimensions and coordinates for the randomly distributed spheres. For the script, the particle/sphere range size considered was between 50 and 200 μm. Also the ratio of inner to outer diameter was maintained constant at 0.9. Besides, all spheres were confined in the given volume and did not overlap with each other. After obtaining the dimensions and coordinates, a CAD model was developed.

5.2.3 Simulation

Using the output obtained from running the MATLAB script, a CAD model was developed. As mentioned previously, a total 1% or 2% deflection was applied, depending on the

model. Since only RVEs were modeled, symmetry was considered when applying boundary conditions. Figure 5.3 depicts the boundary conditions applied to the linear-elastic model. Deflection was applied on the top face (y-direction) of the element while the bottom face was restricted of any motion. The back left face motion was restricted in the x-direction and the back right face motion was restricted in the z-direction. For all models, mesh sensitivity study was conducted to eliminate the possibility of any mesh dependence of the model.

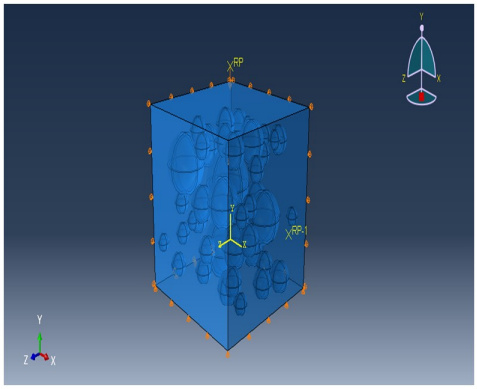

Figure 5.1: Boundary Conditions for Computational Model

The properties used for the 3D model simulation are depicted in Table 5.1. Only the modulus of elasticity and Poissons ratio were input as material properties [84].

Table 5.1: Material properties inputs of matrix and cenospheres.

Material	Modulus of Elasticity (GPa)	Poissons Ratio
Lapox L-12 epoxy resin with K-6 hardener	3.4	0.425
Cenospheres	55	0.19

5.3 Results and Discussion

5.3.1 Linear-Elastic Model

The results for the 20 vol. % model are depicted in Table 5.2. It can be observed that % difference from the modulus of elasticity obtained from the computational model and the experimental values for the same volume fraction represent less than 5%. Using the properties previously discussed, a 2.4% difference between experimental modulus and 1 mm model was achieved. Given that the change in modulus of elasticity was small with respect to each model size, the model size of 0.75 mm was selected to be used for 40 vol. %.

Table 5.2: Computational values obtained for modulus of elasticity for the 20 vol. % model.

Model size(cm)	Modulus of Elasticity (MPa)	% Difference (Error)
0.25	4128.56	4.8
0.50	4070.68	3.3
0.75	4030.54	2.3
1.00	4033.96	2.4

[1]*Exp. Modulus - 3939.28 MPa

As it can be seen in Figure 5.2, the initial slope of the stress-strain curve obtained from computational simulations follows the same trend as experimental data. The difference in the modulus of elasticity between experimental data and the computational model, regardless of the size of the model, was less than 5%. For both volume fractions considered, the model correctly simulates the linear elastic behavior of syntactic foams when subjected to compression.

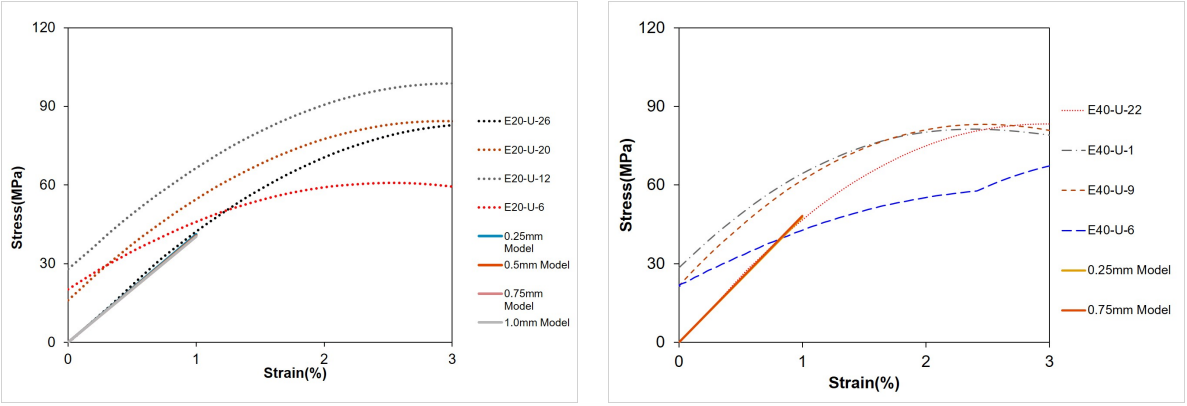

(a) (b)

Figure 5.2: Experimental versus Computational Data for (a)20 vol. % and (b)40 vol.%

In order to determine the influence that the distribution of spheres inside the matrix has in the modulus of elasticity in our model, a packing study was developed using the 40 vol. % model. All models contained different packing and number of spheres but volume fraction remained constant. Table 5.3 show the values obtained for each model. The difference observed was less that 4% for all cases.

Table 5.3: Packing Study: Computational values obtained for modulus of elasticity for the 40 vol. % models.

Model Id.	Modulus of Elasticity (MPa)	% Difference (Error)
1	4832.36	2.88
2	4850.01	3.25
3	4864.07	3.55
4	4855.88	3.37

[2]*Exp. Modulus - 4855.876 MPa

In Figure 5.3, the four distinct packing of the cenospheres developed are compared to each other. It was observed that the modulus of elasticity remains relative constant despite the different distribution of spheres. The distribution of spheres inside the model had

minimal to no effect in the modulus of elasticity of the computational model.

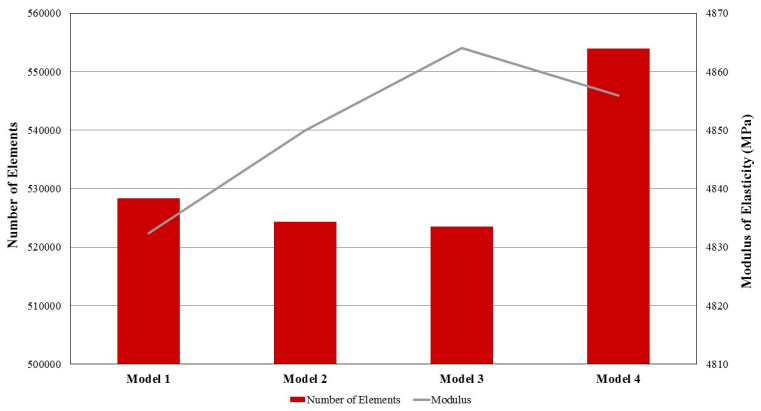

Figure 5.3: Packing Study for 40 vol.% Model

5.3.2 Damage Prediction Model

For the case of the damage prediction model, a 2D model was develop due to the complexity of modeling damage/plasticity. ABAQUS was use for the simulation. The model consisted of 5 spheres with a 20 vol. % and a ratio of inner to outer diameter of 0.9. In order to reduce computational time, mesh refinement around the area of interest was performed as observed in Figure 5.4. In order to account for the damage in the model, cohesive elements with the application of Traction-Separation Laws for damage prediction were used. This elements were used given that once the interface has failed, the surfaces do not re-bond. As opposed to the Linear-Elastic model previously discussed, the model inputs were not the traditional material properties. Instead, stiffness penalties were used as inputs in the model, along with damage initiation criteria and evolution. All the values were tuned individually in order to obtained the corresponding values for each material.

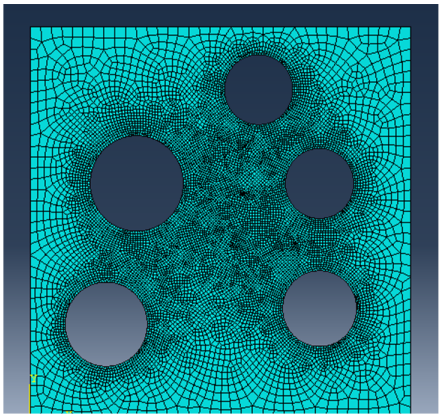

Figure 5.4: Mesh distribution for the 2D damage prediction model (40 vol.%).

In Figure 5.5, the response of the computational model can be observed with respect to experimental values. The model depicts the initial stage of damage. The modulus of elasticity obtained was of 3793.10 MPa, which represent a decrease of 3.7% with respect to experimental values (3939.28 MPa). The model shows close agreement during the linear-elastic region of the curve but as damage starts to developed in the model, the curve deviate from the experimental values.

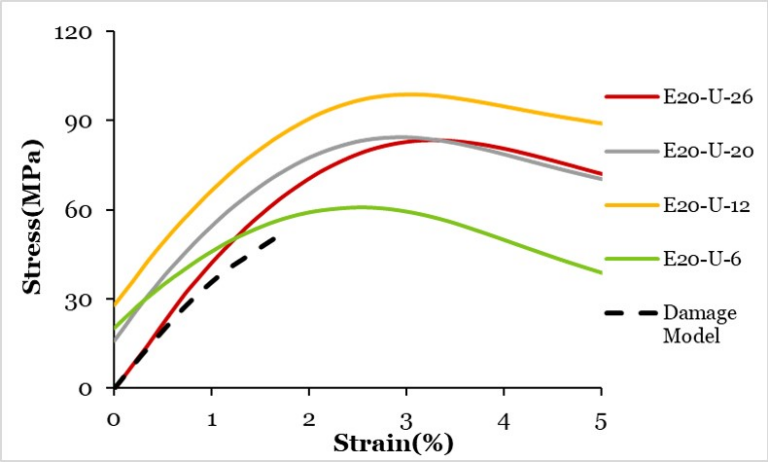

Figure 5.5: Stress-Strain curve comparing experimental versus computational 2D damage prediction model (20 vol.%).

For this case, perfect bonding was assumed between both constituents of the syntactic foam. The damage in the model is observed by the extent of degradation of the cohesive elements. In Figure 5.6, initial crack formation can be observed along the interphase between the matrix and the cenospheres. This crack formations will eventually propagate and lead to the complete failure of the model. In the schematic, it is noticeable that the main crack formations are in this interphase region meaning that material behavior closely depends in the interaction between matrix and spheres.

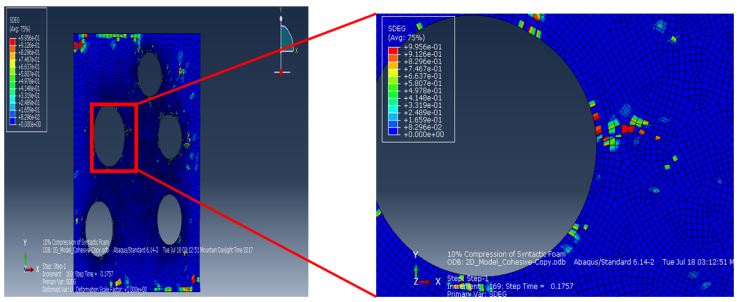

Figure 5.6: Schematic of elements degradation for the computational 2D damage prediction model (20 vol.%).

5.4 Conclusion

A three dimensional computational model was developed to successfully represent the linear-elastic behavior for distinct volume fractions. It was observed that the behavior of the model was similar for all size model within the same volume fraction meaning that the computational model was not dependent on the size or number of spheres included in the syntactic foams. All cases showed closed agreement with the experimental data previously obtained for the epoxy/cenospheres syntactic foam. For the case of the damage prediction model, a two dimensional model was developed capable to model initial damage stages such as crack formation and partial crack propagation. The model demonstrated

close agreement during the linear-elastic region compared to experimental results. The model can serve as a tool to observed the areas where syntactic foams will most likely fail and be able to develop material with superior properties.

Chapter 6

Conclusion and Future Work

6.1 Conclusion

This thesis examined the feasibility of using distinct foam cores for arctic exploration, such as Polyvinyl Chloride (PVC) foams and Cenosphere/Epoxy syntactic foams, by analyzing the impact that the environment might have in the mechanical properties of the material. In all cases, materials were exposed to the worst possible conditions since the core are not in direct contact with the environment. These two type of foam cores were selected due to its low density and small moisture absorption making them ideal for marine applications. For the case of the PVC foams, they were exposed to a combination of scenarios were it included sea water exposure, arctic temperature exposure, and a combined exposure between sea water and arctic temperature exposure. It was observed that room temperature compressive properties in general appear to decrease in conditioned foams, but increased at -60^{o}C. This is attributed to the rigidity imparted to the samples due to freezing at arctic temperatures. Furthermore, room temperature compressive strength and modulus of arctic conditioned foams (DAR) decreased by about 7% and 10%, respectively, which is attributed to the freeze-thaw effect. in general, it was noted that long term sea water conditioning along with arctic exposure is detrimental to the mechanical properties of PVC foams. For the case of Cenosphere/Epoxy syntactic foams, it was determined that all foam compositions show an increase in compressive modulus compared to that of the neat resin at room temperature. In the other hand, the modulus of elasticity decreased for arctic specimens while its compressive strength increased in comparison to the unconditioned (dry) specimens. For the flexural specimens tested at room temperature, it is observed that the flexural strength decreases as the filler content increases. Furthermore, arctic exposed samples reported a slight increase in its modulus of elasticity. In general, all

cenosphere/epoxy foams with treated and untreated fillers exposed to arctic conditions, either for flexural or compressive testing, demonstrated lower failure strains compared to neat epoxy.

6.2 Future work

The study presented demonstrated the influence that a harsh environment, in this case arctic condition, may have core materials used for the elaboration of sandwich composites. The work accomplished in this study will be followed by the following future work:

- Response of Epoxy/Cenosphere under the influece of a combine conditioning between sea water and arctic temperature(-60°C).
- Analysis of different matrix constituent in the fabrication of syntactic foams and the impact when subjected under arctic conditioning.
- Develop computational model capable of including damage and until complete failure in the model behavior.

References

[1] W. Roeseler, Branko Sarh, and M. Kismarton. Composite structures: The first 100 years. *16th International Conference on Composite Materials*, pages 1–10, 2013.

[2] E. Barbero. *Introduction to Composite Materials Design*. Taylor and Francis, 6000 Broken Sound Parkway, 1 edition, 1998.

[3] D. Luong, D. Pinisetty, and N. Gupta. Compressive properties of closed-cell polyvinyl chloride foams at low and high strain rates: Experimental investigation and critical review of state of the art. *Composites: Part B*, 44(2):403–416, 2013.

[4] I.M. Daniel and J.-M. Cho. Characterization of Anisotropic Polymeric Foam Under Static and Dynamic Loading. *Experimental Mechanics*, 51:1395–1403, February 2011.

[5] D.C. Loup, R.C. Matteson, and A.W.J. Gielen. *Material Characterization of PVC Foam under Static and Dynamic Loading*, pages 87–96. Springer Netherlands, Dordrecht, 2005.

[6] L. J. Gibson and M. F. Ashby. *Cellular Solids: Structure and Properties*. Cambridge University Press, July 1999.

[7] K Kanny, H. Mahfuz, L.A. Carlsson, T. Thomas, and S. Jeelani. Dynamic mechanical analyses and flexural fatigue of pvc foams. *Composite Structures*, 58(2):175 – 183, 2002.

[8] F. Aviles and M. Aguilar-Montero. Moisture Absorption in Foam-Cored Composite Sandwich Structures. *Polymer Composites*, 31(4):714–722, 2010.

[9] C.H. Shen and G. S. Springer. Moisture Absorption and Desorption of Composite Materials. *Journal of Composite Materials*, 10(1):2–20, January 1976.

[10] G. Tagliavia, M. Porfiri, and N. Gupta. Influence of Moisture Absorption on flexural properties of syntactic foams. *Composites Part B: Engineering*, 43(3):115 – 123, 2012.

[11] A. Siriruk, D. Penumadu, and A. Sharma. Effects of Seawater and Low temperatures on Polymeric Foam Core Material. *Experimental Mechanics*, 52(1):25–36, 2011.

[12] C. Nordin, Z. J. M.ASCE Ma, and D. M.ASCE Penumadu. Combined Effect of Loading and Cold temperature on the Stiffness of Glass Fiber Composites. *Journal of Composites for Construction*, 14(2):224–230, 2010.

[13] R. L. Sadler, M. Sharpe, R. Panduranga, and K. Shivakumar. Water immersion effect on swelling and compression properties of Eco-Core, PVC foam and balsa wood. *Composite Structures*, 90(3):330–336, January 2009.

[14] CS Karthikeyan, Kishore, and S Sankaran. Effect of absorption in aqueous and hygrothermal media on the compressive properties of glass fiber reinforced syntactic foam. *Journal of Reinforced Plastic Composites*, 20(11):982–993, January 2001.

[15] A. Singh and B. Davidson. Effects of temperature, seawater and impact on the strength, stiffness, and life of sandwich composites. *Journal of Reinforced Plastics and Composites*, 30(3):269–277, March 2011.

[16] DIAB. Divinycell H technical manual. *Laholm, Sweden*, 2016.

[17] ASTM C365/C365M-11a. Standard Test Method for Flatwise Compressive Properties of Sandwich Cores. *ASTM International*, 2011.

[18] ASTM C272/C272M-12. Standard Test Method for Water Absorption of Core Materials for Sandwich Construction. *ASTM International*, 2012.

[19] ASTM D5229-14. Standard Test Method for Moisture Absorption Properties and Equilibrium Conditioning of Polymer Matrix Composite Materials. *ASTM International*, 2014.

[20] ASTM D1141-98. Standard practice for the preparation of substitute ocean water. *ASTM International, West Conshohocken, PA*, 2013.

[21] A. May-Pat and F. Avils. Long term water uptake of a low density polyvinyl chloride foam and its effect on the foam microstructure and mechanical properties. *Materials and Design*, 57:728–735, January 2014.

[22] N. Petchwattana, S. Covavisaruch, and D. Pitidhammabhorn. Influences of water absorption on the properties of foamed poly(vinyl chloride)/rice hull composites. *Journal of Polymer Research*, 20(6):172, June 2013.

[23] F. Shutov. Syntactic polymer foams. In *Chromatography/Foams/Copolymers*, volume 73/74, pages 63–123, 1986.

[24] L. Bardella and F. Genna. Elastic design of syntactic foamed sandwiches obtained by filling of three-dimensional sandwich-fabric panels. *International Journal of Solids and Structures*, 38(2):307333, 2001.

[25] B. Zhu, J. Ma, J. Wang, J. Wu, and D. Peng. Thermal, dielectric and compressive properties of hollow glass microsphere filled epoxy-matrix composites. *Journal of Reinforced Plastics and Composites*, 31(19):1311–1326, 2012.

[26] K.C. Yung, B.L. Zhu, T.M. Yue, and C.S. Xie. Preparation and properties of hollow glass microsphere-filled epoxy-matrix composites. *Composites Science and Technology*, 69(2):260–264, 2009.

[27] R.L. Poveda, G. Dorogokupets, and N. Gupta. Carbon nanofiber reinforced syntactic foams: Degradation mechanism for long term moisture exposure and residual compressive properties. *Polymer Degradation and Stability*, 98(10):2041–2053, 2013.

[28] N. Gupta, B. Singh Brar, and E. Woldesenbet. Effect of filler addition on the compressive and impact properties of glass fibre reinforced epoxy. *Bulletin of Materials Science*, 24(2):219–223, 2001.

[29] B. Satapathy, A. Das, and A. Patnaik. Ductile-to-brittle transition in cenosphere-filled polypropylene composites. *Journal of Materials Science*, 46(6):1963–1974, 2011.

[30] J. Qiao and G. Wu. Tensile properties of fly ash/polyurea composites. *Journal of Materials Science*, 46(11):3935–3941, 2011.

[31] B.R. Bharath Kumar, M. Doddamani, S.E Zeltmann, N. Gupta, M.R. Ramesh, and S. Ramakrishna. Processing of cenosphere/hdpe syntactic foams using an industrial scale polymer injection molding machine. *Materials and Design*, 92:414423, 2016.

[32] N. Gupta, R. Ye, and M. Porfiri. Comparison of tensile and compressive characteristics of vinyl ester/glass microballoon syntactic foams. *Composites Part B: Engineering*, 41(3):236–245, 2010.

[33] G. Gladysz, B. Perry, G. McEachen, and J. Lula. Three-phase syntactic foams: structure-property relationships. *Journal of Materials Science*, 41(13):4085–4092, 2006.

[34] V.C. Shunmugasamy, D. Pinisetty, and N. Gupta. Viscoelastic properties of hollow glass particle filled vinyl ester matrix syntactic foams: effect of temperature and loading frequency. *Journal of Materials Science*, 48(4):1685–1701, 2013.

[35] V.C. Shunmugasamy, D. Pinisetty, and N. Gupta. Electrical properties of hollow glass particle filled vinyl ester matrix syntactic foams. *Journal of Materials Science*, 49(1):180–190, 2014.

[36] N. Gupta, E. Woldesenbet, and P. Mensah. Compression properties of syntactic foams: effect of cenosphere radius ratio and specimen aspect ratio. *Composites Part A: Applied Science and Manufacturing*, 35(1):103–111, 2004.

[37] R. Maharsia, N. Gupta, and H.D. Jerro. Investigation of flexural strength properties of rubber and nanoclay reinforced hybrid syntactic foams. *Materials Science and Engineering: A*, 417(1-2):249–258, 2006.

[38] G. Tagliavia, M. Porfiri, and N. Gupta. Analysis of flexural properties of hollow-particle filled composites. *Composites Part B: Engineering*, 44(6):1462–1468, 2010.

[39] G. Tagliavia, M. Porfiri, and N. Gupta. Influence of moisture absorption on flexural properties of syntactic foams. *Composites Part B: Engineering*, 43(2):115–123, 2012.

[40] W.-H. Lin and M.-H.R. Jen. Manufacturing and mechanical properties of glass bubbles/epoxy particulate composite. *Journal of Composite Materials*, 32(15):1356–1390, 1998.

[41] Kishore, R. Shankar, and S. Sankaran. Short beam three point bend tests in syntactic foams. part i: Microscopic characterization of the failure zones. *Journal of Applied Polymer Science*, 98(2):673–679, 2005.

[42] Kishore, R. Shankar, and S. Sankaran. Short-beam three-point bend tests in syntactic foams. part ii: Effect of microballoons content on shear strength. *Journal of Applied Polymer Science*, 98(2):680–686, 2005.

[43] Kishore, R. Shankar, and S. Sankaran. Short-beam three-point bend test study in syntactic foam. part iii: Effects of interface modification on strength and fractographic features. *Journal of Applied Polymer Science*, 98(2):687–693, 2005.

[44] N. Gupta, Kishore, E. Woldesenbet, and S. Sankaran. Studies on compressive failure features in syntactic foam material. *Journal of Materials Science*, 36(18):4485–4491, 2001.

[45] N. Gupta, E. Woldesenbet, and Kishore. Compressive fracture features of syntactic foams-microscopic examination. *Journal of Materials Science*, 37(15):3199–3209, 2002.

[46] C.S. Karthikeyan, S. Sankaran, M.N. Jagdish Kumar, and Kishore. Processing and compressive strengths of syntactic foams with and without fibrous reinforcements. *Journal of Applied Polymer Science*, 81(2):405–411, 2001.

[47] E. Rizzi, E. Papa, and A. Corigliano. Mechanical behavior of a syntactic foam: experiments and modeling. *International Journal of Solids and Structures*, 37(40):5773–5794, 2000.

[48] J.R.M. d'Almeida. An analysis of the effect of the diameters of glass microspheres on the mechanical behavior of glass-microsphere/epoxy-matrix composites. *Composites Science and Technology*, 59(14):2087–2091, 1999.

[49] P. Bunn and J.T. Mottram. Manufacture and compression properties of syntactic foams. *Composites*, 24(7):565–571, 1993.

[50] N. Gupta and E. Woldesenbet. Hygrothermal studies on syntactic foams and compressive strength determination. *Composite Structures*, 61(4):311–320, 2003.

[51] C.S. Karthikeyan and S. Sankaran. Effect of absorption in aqueous and hygrothermal media on the compressive properties of glass fiber reinforced syntactic foam. *Journal of Reinforced Plastics and Composites*, 20(11):982–993, 2001.

[52] O. Ishai, C. Hiel, and M. Luft. Long-term hygrothermal effects on damage tolerance of hybrid composite sandwich panels. *Composites*, 26(1):47–55, 1995.

[53] H.S. Kim and M.A. Khamis. Fracture and impact behaviours of hollow microsphere/epoxy resin composites. *Composites Part A: Applied Science and Manufacturing*, 32(9):1311–1317, 2001.

[54] S.E. Zeltmann, B.R. Bharath Kumar, M. Doddamani, and N. Gupta. Prediction of strain rate sensitivity of high density polyethylene using integral transform of dynamic mechanical analysis data. *Polymer*, 101:1–6, 2016.

[55] S.E. Zeltmann, K.A. Prakash, M. Doddamani, and N. Gupta. Prediction of modulus at various strain rates from dynamic mechanical analysis data for polymer matrix composites. *Composites Part B: Engineering*, 120:27–34, 2017.

[56] F. Grosjean, N. Bouchonneau, D. Choqueuse, and V. Sauvant-Moynot. Comrehensive analyses of yntactic foam behaviour in deepwater environment. *Journal of Materials Science*, 44(1):86–93, 2009.

[57] S. Guhanathan, M.s. Devi, and V. Murugesan. Effect of coupling agents on the mechanical properties of fly ash/polyester particulate composites. *Journal of Applied Polymer Science*, 82(7):1755–1760, 2001.

[58] B.R. Bharath Kumar, M. Doddamani, S. Zeltmann, N. Gupta, Uzma, S. Gurupadu, and R.R.N. Sailaja. Effect of particle surface treatment and blending method on flexural properties of injection-molded cenosphere/hdpe syntactic foams. *Journal of Materials Science*, 51(8):37933805, 2016.

[59] B.R. Bharath Kumar, S.E. Zeltmann, M. Doddamani, N. Gupta, Uzma, S. Gurupadu, and R.R.N. Sailaja. Effect of cenosphere surface treatment and blending method on the tensile properties of thermoplastic matrix syntactic foams. *Journal of Applied Polymer Science*, 133(35):43881, 2016.

[60] L. Zhang and J. Ma. Effect of coupling agent on mechanical properties of hollow carbon microsphere/phenolic resin syntactic foam. *Composites Science and Technology*, 70(8):1265–1271, 2010.

[61] L. Yusriah and M. Mariatti. Effect of hybrid phenolic hollow microsphere and silica-filled vinyl ester composites. *Journal of Composite Materials*, 47(2):169–182, 2013.

[62] M. Aureli, M. Porfiri, and N. Gupta. Effect of polydispersivity and porosity on the elastic properties of hollow particle filled composites. *Mechanics of Materials*, 42(7):726–739, 2010.

[63] G. Tagliavia, M. Porfiri, and N. Gupta. Analysis of hollow inclusionmatrix debonding in particulate composites. *International Journal of Solids and Structures*, 47(16):2164–2177, 2010.

[64] M.C. Boyce, D.M. Parks, and A.S. Argon. Large inelastic deformation of glassy polymers. part i: rate dependent constitutive model. *Mechanics of Materials*, 7(1):15–33, 1988.

[65] L. Bardella. A phenomenological constitutive law for the nonlinear viscoelastic behaviour of epoxy resins in the glassy state. *European Journal of Mechanics - A/Solids*, 20(6):907–924, 2001.

[66] D.K. Balch and D.C. Dunand. Load partitioning in aluminum syntactic foams containing ceramic microspheres. *Acta Materialia*, 54(6):1501–1511, 2006.

[67] E. Woldesenbet, N. Gupta, and H.D. Jerro. Effect of microballoon radius ratio on syntactic foam core sandwich composites. *Journal of Sandwich Structures and Materials*, 7(2):95–111, 2005.

[68] N. Gupta, S. Zeltmann, V. Shunmugasamy, and D. Pinisetty. Applications of polymer matrix syntactic foams. *JOM*, 66(2):245–254, 2014.

[69] L. Bardella, F. Malanca, P. Ponzo, A. Panteghini, and M. Porfiri. A micromechanical model for quasi-brittle compressive failure of glass-microballoons/thermoset-matrix syntactic foams. *Journal of the European Ceramic Society*, 34:2605–2616, 2014.

[70] L. Bardella, F. Malanca, P. Ponzo, A. Panteghini, and M. Porfiri. Global sensitivity analysis for the elastic properties of hollow spheres filled syntactic foams using high dimensional model representation method. *Computational Materials Science*, 61:89–98, 2012.

[71] R.L. Poveda, S. Achar, and N. Gupta. Viscoelastic properties of carbon nanofiber reinforced multiscale syntactic foam. *Composites Part B: Engineering*, 58:208–216, 2014.

[72] R.L. Poveda and N. Gupta. Carbon-nanofiber-reinforced syntactic foams: Compressive properties and strain rate sensitivity. *JOM*, pages 1–12, 2013.

[73] B.R. Bharath Kumar, A.K. Singh, M. Doddamani, D.D. Luong, and N. Gupta. Quasi-static and high strain rate compressive response of injection-molded cenosphere/hdpe syntactic foam. *JOM*, 68:TBD, in press, 2016.

[74] B.R. Bharath Kumar, M. Doddamani, S.E. Zeltmann, N. Gupta, M.R. Ramesh, and S. Ramakrishna. Data characterizing tensile behavior of censophere/hdpe syntactic foam. *Data in Brief*, page Submitted, 2015.

[75] N.R. Schott and T.K. Bhattacharjee. Journal of cellular plastics. *JOM*, 29(6):556–568, 1993.

[76] M. Palumbo and E. Tempesti. On the nodular morphology and mechanical behavior of a syntactic foam cured in thermal and microwave fields. acta polymerica. *Acta Polymerica*, 49:482–486, 1998.

[77] M. Narkis, M. Puterman, and S. Kenig. Syntactic foams ii. preparation and characterization of three-phase systems. *Journal of Cellular Plastics*, 16(6):326–330, 1980.

[78] J.R. Vinson. Sandwich structures. *Applied Mechanics Reviews*, 54:201–214, 2001.

[79] N. Sharma, R.F. Gibson, and E.O. Ayorinde. Fatigue of foam and honeycomb core composite sandwich structures: A tutorial. *Journal of Sandwich Structures and Materials*, 8:263–319, 2006.

[80] J. Gu, G. Wu, and X. Zhao. Effect of surface-modification on the dynamic behaviors of fly ash cenospheres filled epoxy composites. *Polymer Composites*, 30(2):232–238, 2009.

[81] D.J. Duval, S.H. Risbud, and J.F. Shackelford. Mullite. *Ceramic and Glass Materials*, pages 27–39, 2008.

[82] J.S. Huang and L.J. Gibson. Elastic moduli of a composite of hollow spheres in a matrix. *Journal of the Mechanics and Physics of Solids*, 41(1):55–75, 1993.

[83] N. Gupta and R. Nagorny. Tensile properties of glass microballoon-epoxy resin syntactic foams. *Journal of Applied Polymer Science*, 102:1254–1261, 2006.

[84] M. Doddamani, Kishore, V.C. Shunmugasamy, N. Gupta, and H.B. Vijayakumar. Compressive and flexural properties of functionally graded fly ash cenosphere/epoxy resin syntactic foams. *Polymer Composites*, 36(4):685–693, 2015.

[85] P. R Marur. Numerical estimation of effective elastic moduli of syntactic foams. *Finite Elements in Analysis and Design*, 46:1001–1007, 2010.

[86] F.V. Antunes, J.A.M. Ferreira, and C. Capela. Numerical modelling of the youngs modulus of syntactic foams. *Finite Elements in Analysis and Design*, 47:78–84, 2011.

Curriculum Vitae

Carlos Daniel Garcia Perez was born in Ciudad Juarez, Chihuahua, Mexico. He started college at the University of Texas at El Paso in the fall of 2012. After three years, he received his bachelors degree in Mechanical Engineering. He graduated as part of the top ten mechanical engineering students along with receiving institutional honor - Summa Cum Laude.

In Spring 2016, he entered the Graduate School at the University of Texas at El Paso, where he will be earning his Masters degree in Mechanical Engineering in Summer 2017. There he has worked as a Undergraduate Level Advisor and Research Assistant while pursuing his masters degree. His research interests are focused on the response of foam core materials for sandwich composites under extreme conditions.

Contact Information: cdgarcia3@miners.utep.edu